A multi-objective optimisation framework for the design of ship energy systems under operational and environmental uncertainty

Vasilikis, Nikolaos; Geertsma, Rinze; Coraddu, Andrea

DOI
10.1016/j.apenergy.2025.126829

Publication date
2025

Document Version
Final published version

Published in
Applied Energy

Citation (APA)
Vasilikis, N., Geertsma, R., & Coraddu, A. (2025). A multi-objective optimisation framework for the design of ship energy systems under operational and environmental uncertainty. *Applied Energy*, *402*, Article 126829. https://doi.org/10.1016/j.apenergy.2025.126829

Applied Energy 402 (2025) 126829

Contents lists available at ScienceDirect

Applied Energy

journal homepage: www.elsevier.com/locate/apen

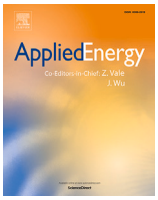

A multi-objective optimisation framework for the design of ship energy systems under operational and environmental uncertainty

Nikolaos Vasilikis [a,*], Rinze Geertsma [b,a], Andrea Coraddu [a,b]

[a] Department of Maritime and Transport Technology, Delft University of Technology, Delft, the Netherlands
[b] Faculty of Military Sciences, Netherlands Defence Academy, Den Helder, the Netherlands

HIGHLIGHTS

- Use of discretised probability distributions of actual sailing profiles of sister ships.
- A framework that considers environmental, financial and technical objectives.
- A modelling approach that allows for extensive design space exploration.
- A solver combining a genetic algorithm and interior point method in a multi-start scheme.
- Calm water and typical design assumptions misleading in life-cycle assessments.

ARTICLE INFO

Keywords:
Optimisation under uncertainty
Multi-objective optimisation
Mixed-integer nonlinear programming
Ship energy systems
EEDI

ABSTRACT

Hybrid propulsion is considered a reliable alternative to solely mechanical or electrical propulsion for enhanced ship energy performance. Nevertheless, an increased number of components and interconnections results in more complex ship design problems. The automotive and aviation industries already examine new designs on predefined driving and flying cycles. However, new ships are still assessed on one design point with the regulated Energy Efficiency Design Index (EEDI). Its limited consideration of calm water conditions and installed rated power is characterised as insufficient, if not dangerous. A design methodology that accounts for operational and environmental uncertainty is lacking. This paper proposes a design optimisation framework for the topology selection and sizing of hybrid propulsion systems integrating probability distributions of actual sailing profiles from continuous monitoring. The methodology is demonstrated on the 'Holland' class ocean patrol vessels of the Royal Netherlands Navy. Its multi-objective consideration examines a wide design space from an environmental, financial, and technical perspective, solving the mixed-integer nonlinear programming (MINLP) problem with a multi-starting scheme that combines a genetic algorithm and interior point method. The low computational cost is achieved by integrating a state-of-the-art digital twin approach leveraging data-driven and first-principle modelling. The results demonstrate feasible improvements of approximately 4 % for carbon intensity and 11 % for operational expenditure by increasing the size of the electrical motors. The exact configuration and percentage improvement are sensitive to actual operational and environmental conditions, while calm water conditions tend to overestimate savings. Consequently, the use of actual sailing profiles is recommended for more accurate life-cycle predictions.

1. Introduction

The maritime industry still delivers more than 80 % of global trade, overcoming fluctuations caused by the COVID-19 pandemic [1]. Despite the large scale of operations, the International Maritime Organization (IMO) decided to strengthen its greenhouse gas (GHG) reduction strategy, moving from the initial goal of cutting emissions by half by 2050 [2] to a new target of achieving net-zero emissions around the same period [3]. In many cases, electrification of ships has been identified as the way forward, though a solely electrical propulsion system suffers from a number of disadvantages with the increased conversion losses near top ship speed being the most prominent [4]. Hybrid propulsion systems are considered a reliable alternative, though the correct

* Corresponding author.
Email address: nikolaos.vasilikis@gmail.com (N. Vasilikis).

https://doi.org/10.1016/j.apenergy.2025.126829
Received 3 June 2025; Received in revised form 14 September 2025; Accepted 26 September 2025
Available online 16 October 2025

Table 1
Acronyms and symbols.

Acronym	Description
IMO	International Maritime Organization
EEDI	Energy efficiency design index
WLTC	World-wide harmonized light duty test cycle
LTO	Landing and take-off cycle
CCD	Climb, cruise, descend cycle
NPV	Net present value
IPMS	Integrated platform monitoring system
MINLP	Mixed-integer non linear programming
MOCO	Multi-objective combinatorial optimisation
GA	Genetic algorithm
CAPEX	Capital expenditure
OPEX	Operational expenditure
IRR	Internal rate of return
GHG	Greenhouse gas
NO_x	Nitrogen oxides
SO_x	Sulphur oxides
PM	Particulate matter
WHR	Waste heat recovery
RNLN	Royal Netherlands navy
ISO	International organization for standardization
EMS	Energy management strategy
Symbol	**Description**
v	Vessel speed
T	Total propeller thrust
T_{air}	Ambient air temperature
$p(v,T)$	Probability of occurrence for the corresponding pair (v,T)
$\mathbf{x}$	Vector of independent decision variables
$\mathbf{x}_{\text{ga}}$	The solution of the genetic algorithm
$\mathbf{x}_{\text{best}}$	The best solution out of all genetic algorithm starts
$\mathbf{x}^*$	The solution of the optimisation algorithm
$\mathbf{p}$	Vector of fixed parameters describing the examined system
$\mathcal{I}$	Optimisation input scenario
CI	Carbon intensity
C_{capex}	Capital expenditure cost
C_{opex}	Operational expenditure cost
W_{tot}	Total weight of the considered system
λ	Weight expressing the importance of different objectives
C_{maint}	Maintenance cost
c_{e}	Purchase cost coefficient of main diesel engines
c_{g}	Purchase cost coefficient of diesel generators
c_{m}	Purchase cost coefficient of electrical motors
c_{μ}	Maintenance cost coefficients
i_{f}	Inflation rate
i_{m}	Market interest
N_{y}	Years under consideration
P_{e}	Main diesel engine rated power
P_{gen}	Diesel generators rated power
P_{hotel}	Hotel electrical power
P_{m}	Electrical motors nominal power rating
N_{a}	Type a diesel generators number
P_{a}	Type a diesel generators rated power
N_{b}	Type b diesel generators number
P_{b}	Type b diesel generators rated power
$\dot{m}_{\text{f,e}}$	Main diesel engines fuel consumption
$\dot{m}_{\text{f,gen}}$	Diesel generators fuel consumption
$\dot{m}_{\text{f,tot}}$	Total fuel consumption
M_{f}	Total amount of consumed fuel
M_{CO2}	Total amount of emitted carbon dioxide

sizing and selection of components is not a simple design problem due to the exploding size of the design space [5].

The energy performance of the majority of new ships is regulated with the Energy Efficiency Design Index (EEDI) [6]. Although the name implies assessing the vessel's energy efficiency, this index provides carbon emissions per transport work, or carbon intensity, on a single sailing point determined by the rated power of main propulsors and a vessel's resistance in calm water conditions. As a consequence, it does not examine part-load energy savings of different hybrid propulsion systems and it does not consider the operational and environmental uncertainty at sea [7]. Additionally, its use in the design of ships instead of actual operating profiles of real ships tends to underestimate the lifetime energy savings of different energy solutions [8]. Other transportation

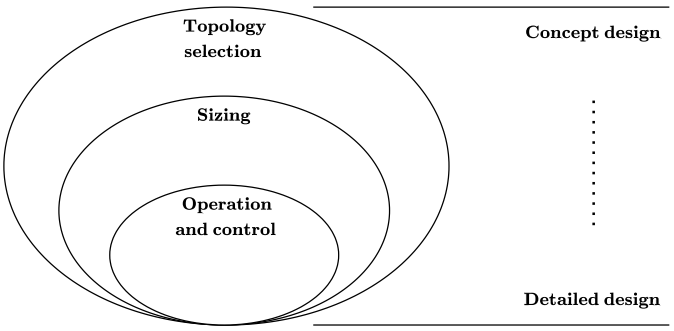

Fig. 1. Optimisation of ship energy systems.

fields such as automotive and aviation point in the same direction, evaluating carbon emissions and fuel economy on driving cycles and flight profiles accordingly [9,10].

The design of ship energy systems involves additional difficulty due to a large number of components, their non-linear behaviour, and interconnection [11,12]. Recently, increasing requirements on ship energy performance impose the design of more complex ship energy systems than in the past as well [4]. A common practice is to design ships according to sets of empirical rules [13]. However, ship design by optimisation has already established its superior performance [14], with the detail and type of problem addressed changing at different design phases [5] as suggested in Fig. 1.

As early as in concept design, energy performance analysis and optimisation problems include topology selection and sizing of propulsion and power supply components [15]. In a later stage, problems involve sizing and energy management [16,17]. Different fuel types and technologies are also examined for the energy transition and maritime decarbonisation [18–20]. Finally, another branch of optimisation problems focuses on the optimal design and operation of specific components such as propellers [21–23], engines [24], and subsystems [25,26]. Regardless of the application, the usual objectives of the optimisation problems can be classified as environmental, social, economic, and technical [27].

Environmental problems usually involve minimising greenhouse gas emissions, mainly carbon dioxide emissions, but also other exhaust gas pollutants, thermal pollution, noise pollution, and land deterioration. The examined time window also varies from static single-point calculations, as in the case of EEDI, to life-cycle assessments that evaluate gas emissions over the building, operation, and dismantling of ships [28]. Finally, minimisation of carbon emissions should not be confused with maximising the energy efficiency of energy systems as demonstrated in [29] and [15], or with reducing nitrogen oxides (NO_x) and sulphur (SO_x) oxides, and primary particulate matter (PM) emissions.

Financial objectives include indicators such as capital expenditure (CAPEX), operational expenditure (OPEX), life-cycle cost (LCC), internal rate of return (IRR), among others. Capital expenditure usually involves purchasing costs, while operational expenditure consists mainly of fuel, lubrication, and maintenance costs [18,26,30]. Recently, with increasing complexity of systems, the cost of replacing batteries is also considered [31]. Last but not least, technical objectives refer to the reserved volume of machine rooms, the total weight of the power supply and propulsion system [19,32,33] or the reserved ballast space [34].

1.1. Related work

Literature provides numerous studies on the design optimisation of ship energy systems [16,17,35]. Taking into account the elements of an optimisation problem, such as the number and nature of objectives, the different simulation scenarios, the case study application itself, and the selected mathematical formulation and solvers, classification can be done in different ways. Since our study focuses on a framework for the design optimisation of hybrid propulsion systems, we categorise literature examples according to application, as shown in Fig. 1.

Purely on topology selection, Livanos et al. [36] compared techno-economic performance using LCC and environmental performance using EEDI for a number of alternatives to the original diesel engine plant of a Ferry/Ro-Ro vessel using steady state models. Again, on topology selection, though optimising the size as well, lies the work by Trivyza et al. [18]. This study examines the simultaneous minimisation of three types of emissions and life cycle cost for a large number of available technologies. It utilises steady state models to simulate operation over a number of operating states and a non-dominated sorting genetic algorithm (NSGA-II) to solve the multi-objective combinatorial optimisation (MOCO) problem. In this direction, Wu et al. [37] also examines a number of different technologies for the case of a medium size cruise ship. Specifically, they solve a net present cost single-objective MINLP problem, and a cost and emissions bi-objective MINLP problem, for typical seasonal power profiles, while focusing on the selection of designs from the Pareto front using the Euclidean distance and data envelopment method.

Solely focused on the sizing of components, Solem et al. [38] optimised a diesel-electric system configuration over a number of working points while considering area size violation as a lost cargo profit in their cost objective. The examined options in their study are actual engine models of different manufacturers, and they solved their problem using the branch-and-bound technique. Sakalis and Frangopoulos [26] optimise the size of main diesel engines by minimising present worth cost (PWC) using a genetic algorithm, although going deeper into modelling in detail exhaust heat treatment. Their analysis manifests the use of genetic algorithms in maritime energy system optimisation problems. Finally, Zhu et al. [39] take extra steps in component sizing by optimising not only the size of electrical motors, diesel generators, and batteries, but also the area of the sail of a sail-hybrid electric power system (sail-HEPS) under the stochastic effect of wind and wave conditions. Annual GHG emissions and LCC are used as objectives, and the problem is solved using multi-objective particle swarm optimisation (MOPSO).

On energy management, Ancona et al. [30] examined load allocation on a diesel mechanical and diesel hybrid system of a cruise ship. The objective function consists of the cost of fuel, maintenance, and the cost of buying electricity from the national grid. Furthermore, they introduce a fictitious regulatory cost to prioritise or penalise certain strategies. Their analysis uses mechanical, electrical, thermal, and cooling hourly power profiles over winter, summer, and spring/autumn. They also use a genetic algorithm and perform a deeper financial investment and environmental analysis on the optimal system obtained. Dedes et al. [40] also optimised power allocation of main diesel engines, diesel generators, and electricity storage means finding the global minimum of fuel consumption between charging and discharging modes. They additionally point out the importance of optimally sizing the system. Finally, Balsamo et al. [41] used dynamic programming to find the optimal battery current of a system that consists of batteries and supercapacitors on a fast craft in order to minimise charging/discharging fluctuations.

Another branch of studies works on both the sizing and energy management of components. Zhu et al. [42] optimised the size of diesel generators and batteries on a hybrid anchor handling tug supply vessel and the energy management rule-based parameters. The tug's operation involves shore charging. What is interesting in their methodology is the modelling of motors and generators' performance of different sizes with the scaling technique of the Willan's line that uses principal dimensions, which they used as design variables. In their subsequent work, they continued their single-objective optimisation work in a bi-objective optimisation problem [43]. Wang et al. [44] also worked on the optimal sizing and control of an examined hybrid system of an offshore support vessel utilising batteries and fuel cells, with the introduction of a double layer optimisation methodology. Specifically, upper-layer optimisation involves the optimal sizing of main diesel engines, batteries, and fuel cells, while the inner layer involves the optimal load allocation. The objectives used in their work are CAPEX, OPEX, and emissions. Finally, Dotto and Satta [45] examined the topology, sizing, and energy management of the hybrid-electric system of a cruise ship powered by natural gas (LNG). Two optimisation steps were also considered. The first step used eight-day phase mean electrical and thermal profiles for topology selection and sizing, while the second used two-day hourly profiles for energy management. The solution algorithm involved piecewise linear consideration for the MINLP problem.

A different category of studies examines systems in more detail and focuses on optimising the working parameters of thermodynamic cycles. For example, Baldi et al. [25] optimised the organic Rankine cycle of a suggested waste heat recovery (WHR) system of a product/chemical tanker. This work contributes to the substantial improvement of energy efficiency by accounting for part-load operation, comparing results on a single design point, a design and part-load point, and the actual power propulsion and auxiliary power profiles over one year. Shu et al. [46] reaches a similar conclusion with the comparison of optimal WHR operation based on six operating conditions and the most frequent (design) condition. Dotto et al. [20] optimised cogeneration efficiency in the case of a large cruise ship, using methanol, ammonia, and methane-hydrogen blends. In their study they used a combined multi-objective genetic algorithm and gradient descent optimiser, and they examined power profiles over five routes, three operating conditions, and a distinction between summer and winter periods. Finally, focusing on the tuning of diesel engines, Tadros et al. [24] minimised the fuel consumption of a four-stroke turbocharged diesel engine by selecting the speed of turbocharger, start angle of injection, intake-valve timing, and amount of injected fuel or combined the performance of a diesel engine and propeller using two distinct optimisation modules [47].

Ship design optimisation problems with a wider scope include the parametric geometry design of the hull and propellers. Design optimisation of propellers, especially controllable-pitch ones, recently focuses on the overall fuel consumption of propulsion systems rather than the energy efficiency of the propeller itself [21–23]. The scenarios examined in their design usually consist of sets of thrust and rotational speed, while genetic algorithms are mainly used as solvers. Optimisation of the hull geometry of cargo vessels [34,48,49], principal dimensioning in the concept design [50], or combined hull and propeller [51,52] provides methodologies for optimal unit transportation cost, resistance, attained speed, required ballast, and building cost. Multi-objective optimisation frameworks consider the uncertainty related to operational and environmental conditions and the main solvers used are genetic algorithm and particle swarm algorithm variants.

1.2. Operational and environmental uncertainty

Ship designers encounter high uncertainty regarding the performance of their implemented designs [52–54]. One way to classify uncertainty in ship design optimisation problems is into uncertainty coming from the environment, the market, and the method/modelling used [34]. In particular, variation in operational and environmental conditions affects the optimisation scenarios and has been shown to be important for the optimal design of ship energy systems [25,39,46,55]. Environmental uncertainty is mainly related to wind and wave conditions, currents, and ambient air and sea temperature, which have a strong geographical and seasonal dependence. Operational uncertainty, on the other hand, is related to the speed of sailing, the loading condition, propeller and hull fouling, and manoeuvring activity.

As discussed in the previous paragraphs, the design point used in the calculation of EEDI is not representative of the operational and environmental uncertainty at sea. Other transportation fields already use driving cycles and flight profiles, like the World-wide harmonized Light duty Test Cycle (WLTC) in automotive [9], or the Landing and Take-off (LTO) and the Climb, Cruise, Descent (CCD) cycles in aviation. Although these cycles are already more detailed than EEDI, emission performance gaps have been observed between real world driving and laboratory testing [56], a gap that following the 'diesel gate' scandal was estimated at 30–40 % [57,58]. For this reason, research in both

automotive and aviation moves in the direction of adopting more realistic running profiles through the statistical analysis of actual driving and flight profiles [59–61]. Latest maritime literature follows this approach with a number of publications either indicating the necessity or aiming to provide such operational profiles [52,62–64].

1.3. Research gap

A common consideration in the design optimisation literature of ship energy systems at a whole system level is a limited number of static points to describe the effect of operational and environmental uncertainty overlooking its effect on obtained results. In an attempt to tackle this, actual power profiles or power profiles that result from the probabilistic consideration of environmental conditions are integrated into problem formulations, although these profiles usually refer to certain components, technologies, and operational decisions and cannot be used to examine different designs.

More specifically on a regulatory basis, EEDI does not account for part-load operation even in the case of multifunction ships—the broader category in which naval vessels could be placed— that are commonly equipped with hybrid propulsion. This means that benefits of using electrical propulsion are only reflected in the attained score if electrical motors contribute to propulsion at the reference design point, which is usually not the case.

Finally, in the selection of objectives, literature provides many examples of using the total life-cycle cost [18,26,36,37,39]. This consideration is sensitive to the selected fuel, maintenance and unit capital costs and does not demonstrate the effect of capital investment on the reduction of carbon footprint and operational costs, which is important for stakeholders in the maritime industry.

1.4. Aim and contribution

This work proposes a novel multi-objective optimisation framework for the topology selection and sizing of hybrid propulsion systems following a physically informed data-driven modelling approach.

The proposed framework adopts discretised probability distributions of actual sailing profiles from the continuous monitoring of three sister ships described by vessel speed and propeller thrust for the following reasons:

- The increased thrust level over calm water resistance at corresponding speed captures the aggregate effect of different operational and environmental conditions.
- It allows the use of more detailed component maps integrating functioning over different shaft speeds compared to power profiles, not only energy efficiencies dependent on power.
- Such vessel operational profiles can be used both with mechanical and electrical propulsion utilising different combinator curves.

As demonstrated in the previous work of the authors [65], a steady-state digital twin leveraging first-principle and operational data-driven techniques that integrates this speed and thrust consideration can be accurate and computationally inexpensive, allowing an extended exploration of the design space that is not limited to the selection of individual components, but extends to the performance modelling of a continuous solution space.

The presented hybrid optimisation algorithm employs a genetic algorithm and interior point method in a multi-start scheme, ensuring the stochastic global exploration of the design space with local deterministic refinement.

This framework considers environmental, financial, and technical objectives with a focus on capital investment returns, it demonstrates a rich set of Pareto optimal designs, and focuses on trade-offs and mechanisms rather than case-specific results.

Finally, in the decision making phase, it adopts a weighted-sum formulation of the multi-objective problem allowing the direct implementation of designer preferences, and it provides the engineering rationale behind the selection of designs from different regions of the Pareto front.

Fig. 2. *Zr. Ms. Holland* ocean patrol vessel (http://www.defensie.nl).

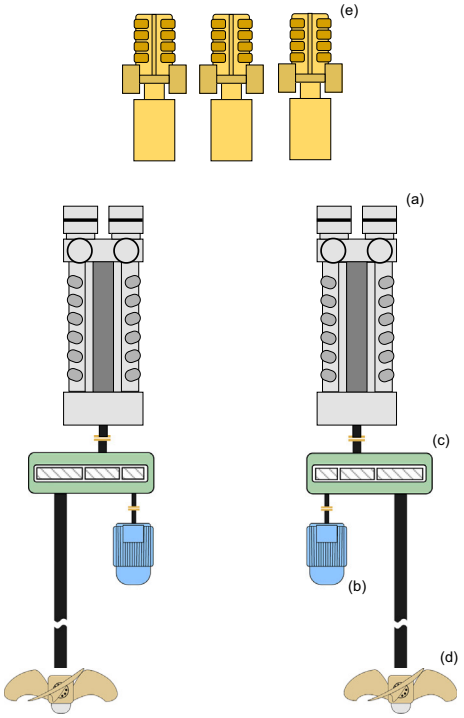

Fig. 3. The original topology of the examined system: (a) main diesel engine, (b) electrical motor, (c) gearbox, (d) controllable-pitch propeller, (e) diesel generator.

The rest of the paper is organised as follows; Section 2 provides an overview of the case study class of vessels, the alternative system designs and the used operational datasets, Section 3 describes the methodology and optimisation framework, Section 4 presents the results for the case of single-objective and multi-objective optimisation, and finally Section 5 provides the conclusions and future work. An overview of the used acronyms and symbols can be found in Table 1.

2. Case study

2.1. Original design

The case study design is the *Holland class* ocean patrol vessels designed by DAMEN Naval for the Royal Netherlands Navy (RNLN) (Fig. 2). A total of four vessels were built between 2008 and 2011. The vessels are equipped with hybrid propulsion as seen in Fig. 3.

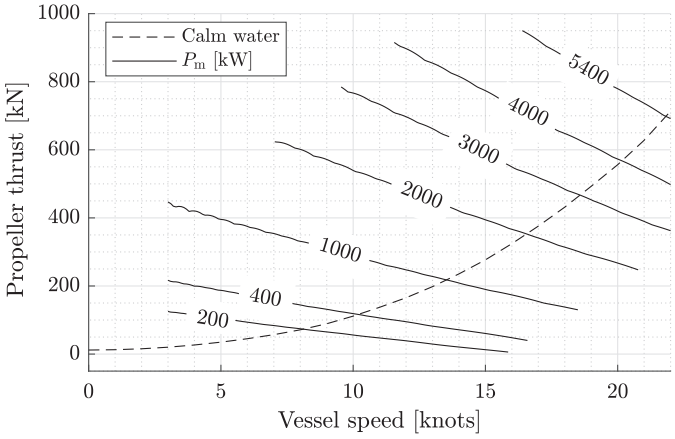

Fig. 4. Maximum thrust limit during electrical propulsion for electrical motors of different size.

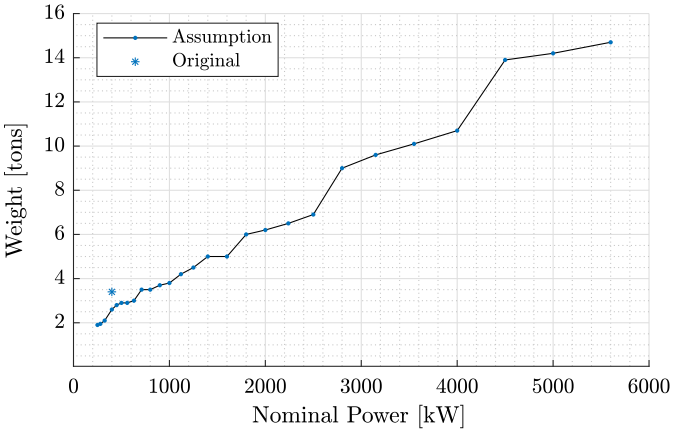

Fig. 5. Weight of the electrical motors on offer.

Two controllable pitch propellers are driven mechanically by two main diesel engines or electrically by two electric motors. Speed is reduced in two two-stage gearboxes, and three diesel generators produce electrical power. The characteristics of the components that are relevant to our study can be found in Table 4.

2.2. Alternative designs

The examined alternative designs include the resizing of the electrical power supply and propulsion of the vessels, adding the power take-off option which allows electrical motors to perform as shaft generators. The main parameter describing the size of the electrical system is the size of the two electrical motors. The vessel is equipped with two low-speed induction motors rated at 400 kW. At this rating, the vessel can sail up to 10 knots in calm water conditions, preventing the main diesel engines from operating at loads lower than 15 %, an operating area that exhibits increased brake specific fuel consumption and results in additional maintenance costs. Electrical propulsion also offers the advantage of reduced noise nuisance. Larger electrical motors would allow the vessels to sail on electrical propulsion at higher speeds, as shown in Fig. 4.

Larger electrical motors can be either low voltage up to approximately 2 200 kW or high voltage above that rating. High-voltage motors for marine applications typically utilise 3 300, 6 600, and 11 000 V, compared to 440 V, and require additional modifications to the power system architecture, such as adding transformers for both the propulsion converters and the mission system and auxiliary loads. It is not within the scope of this study to design a detailed electrical system of the vessel, as this takes place at a more advanced stage of the design process. This range of voltages refers to medium-voltage shore applications. ABB offers a variety of high-frequency electrical motors for marine applications, the weight and rating of which can be found in Fig. 5. Furthermore, these electrical motors can run at lower speeds, comparable to the nominal speed of the main diesel engines of 1 000 rpm. This allows the motors and the main diesel engines to share the same single reduction stage gearbox.

On the electrical power supply, larger motors require greater electricity production. The total electricity production of the current design is 3x910 kW. The specific fuel consumption and weight of different diesel generators available in the market can be found in Figs. 6 and 7. Catalogue-specific fuel consumption of diesel generators has a tolerance of +5 %, usually without engine driven pumps, it refers to fuel of lower calorific value 47 700 kJ/kg, ISO fuels, and ISO standard reference conditions, and it does not include the effect of aging which can cause an increase of up to 2 % [66,67]. Engine-driven pumps can add 2.5 % as well [68]. As a consequence, our study considers a conservative increase of 8 % over the catalogue value to compensate for operation under actual working conditions and non-ISO fuels.

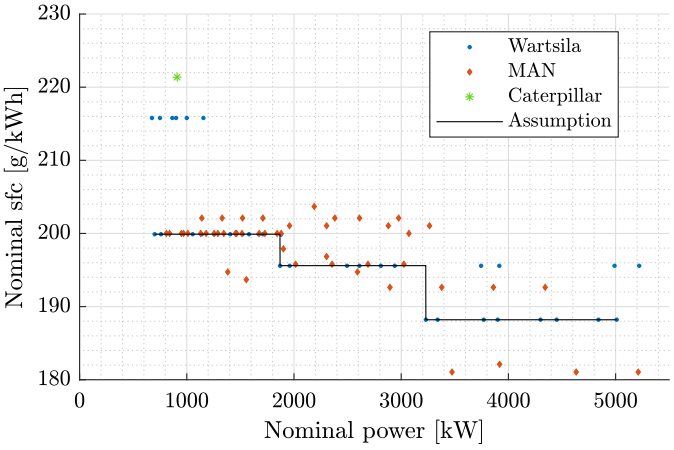

Fig. 6. Catalogue nominal specific fuel consumption of diesel generators on offer.

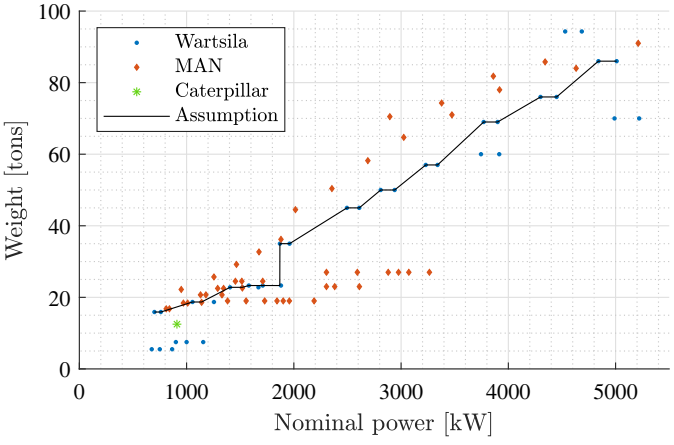

Fig. 7. Weight of the diesel generators on offer.

Table 2
Logged IPMS parameters used.

Parameter	Unit
Main diesel engine speed	[rpm]
Main diesel engine fuel consumption	[kg/h]
Diesel generators speed	[rpm]
Diesel generators power	[kW]
Diesel generators fuel consumption	[kg/h]
Electrical motor speed	[rpm]
Electrical motor power	[kW]
Propeller shaft speed	[rpm]
Propeller shaft torque	[kNm]
Propeller pitch to dimaterer	[-]
Vessel speed through water	[knots]
Propulsion mode	–
Sailing mode	–
Ambient air temperature	[°C]
Relative wind speed	[knots]
Time	[sec]

Table 3
Timespan and sailing days for the three examined vessels.

	Vessel 1	Vessel 2	Vessel 3
Timespan	440	573	958
Sailing time	87	103	131

2.3. Operational datasets

The work carried out in this paper is based on operational data recorded by the Integrated Platform Monitoring System (IPMS) of the vessels. A list of these parameters can be found in Table 2. All parameters are measured by the automation system, except for the thrust parameter, which is estimated based on the dataset enrichment methodology described in earlier work by the authors [29]. Cleaning and pre-processing were performed as in [69], but vessel speed was selected as the primary parameter, excluding values below the 0.1st percentile and above the 99.9th percentile to eliminate outliers instead of using a standard deviation-based approach. The datasets are characterised by a sampling frequency of 3 s and cover a time window as seen in Table 3.

3. Methodology

This paper provides an optimisation framework for the topology selection and sizing of the hybrid propulsion system of ships accounting for operational and environmental uncertainty. This framework evaluates different systems from an environmental, financial, and technical perspective. The simulation of the vessel's operation utilises a state-of-the-art digital twin approach for the modelling of the vessel's energy system leveraging first-principle and operational data-driven techniques developed by the authors in a previous stage [65]. Although computationally expensive to build, this model is sufficiently inexpensive to use in design optimisation applications. The steps of the methodology and the developed framework can be found in Figs. 8 and 9 and are fully described in this section.

3.1. Problem description

As discussed in the introduction of this paper, topology and sizing optimisation have emerged as innovative techniques in the design of ship energy systems, particularly of hybrid systems. Advanced computational methods determine the most efficient and effective layout and size within a specific design space, aiming to achieve the best performance under given constraints. For marine power supply and propulsion systems, this means determining the optimal configuration of components – such as combustion engines, electric motors, energy storage systems, and transmission elements – to ensure seamless power delivery, reduce fuel consumption, and minimise environmental impact. This study concentrates on the optimal design of future classes of ships based on results of analysis and modelling over operational data available from the monitoring of three vessels of the same class that operated under diverse operational and environmental conditions.

Table 4
Original powertrain design associated parameters.

Parameter	Symbol	Value	Unit	Optimised
Main diesel engine nominal power	P_e	5 400	[kW]	
Main diesel engine nominal speed	n_e	1 000	[rpm]	
Gearbox reduction stage 1	r_e	4.355	[-]	
Gearbox reduction stage 2	r_m	17.88	[-]	
Electrical motors nominal power	P_m	400	[kW]	✓
Electrical motors nominal speed	n_m	1788	[rpm]	
Number of type *a* diesel generators	N_a	2		✓
Power rating of type *a* diesel generators	P_a	910	[kW]	✓
Number of type *b* diesel generators	N_b	–		✓
Power rating of type *b* diesel generators	P_b	–	[kW]	✓

Based on the number and type of components, it is possible to define a number of parameters that can be optimised. Some of them will be kept fixed, while some will be optimised as seen in Table 4. The examined problem focuses on the electrical propulsion system of the vessel, hence all new designs considered use the same main diesel engines, propellers, shaft lines and combinator curves. We further assume that mechanical and electrical propulsion use the first reduction stage of the original two-stage reduction gearboxes. New designs will still involve two electrical induction motors. The main design parameters concern the size of the two electrical motors and the number and size of diesel generators. The number of different types of diesel generators is set to two based on common design practice, from now on type a and type b. The performance of different designs is examined under calm water and design conditions, but also on the actual operational and environmental conditions encountered by the three vessels of the class.

3.2. Optimisation problem formalisation

The developed optimisation framework aims to minimise four objectives, namely carbon intensity CI, operational expenditure C_{opex}, capital expenditure C_{capex} and total weight W_{tot}, written as:

$$\min_{\mathbf{x}} \quad \mathrm{CI} \quad (\mathbf{x}, \mathbf{p}, \mathcal{I}), \tag{1}$$

$$\min_{\mathbf{x}} \quad C_{opex}\,(\mathbf{x}, \mathbf{p}, \mathcal{I}), \tag{2}$$

$$\min_{\mathbf{x}} \quad C_{capex}(\mathbf{x}, \mathbf{p}), \tag{3}$$

$$\min_{\mathbf{x}} \quad W_{tot}\ (\mathbf{x}, \mathbf{p}). \tag{4}$$

$\mathbf{x}$ is the vector of design variables:

$$\mathbf{x} = \left(P_m,\ N_a,\ P_a,\ N_b,\ P_b \right), \tag{5}$$

with P_m being the power rating of electrical motors, N_a, P_a, N_b, P_b the number and power rating of diesel generators type a and type b, where:

$$P_m, P_a, P_b \in \mathbb{R} \text{ and } N_a, N_b \in \mathbb{I}, \tag{6}$$

$\mathbf{p}$ are the fixed parameters discussed in the problem description and demonstrated in Table 4, and $\mathcal{I}$ the uncertain optimisation input scenario reflecting the examined operational and environmental conditions. A scenario in the context of this work is described as a set of tuples of vessel speed v, propeller thrust T, the probability of occurrence of each

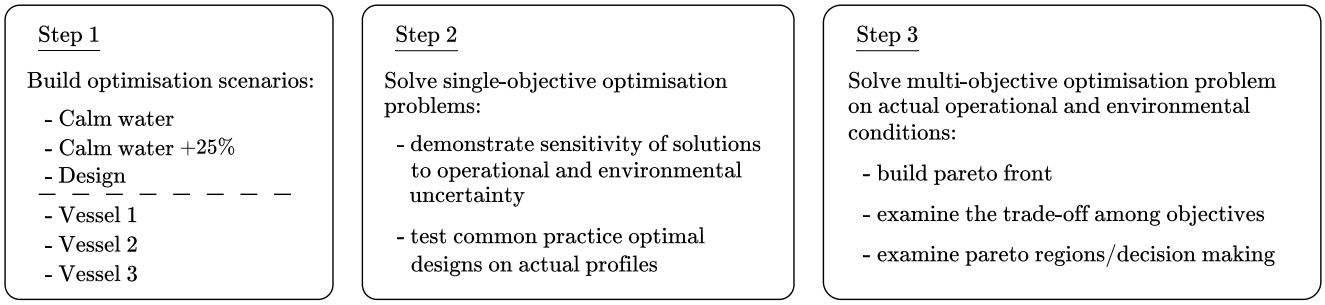

Fig. 8. The methodology steps followed in this paper.

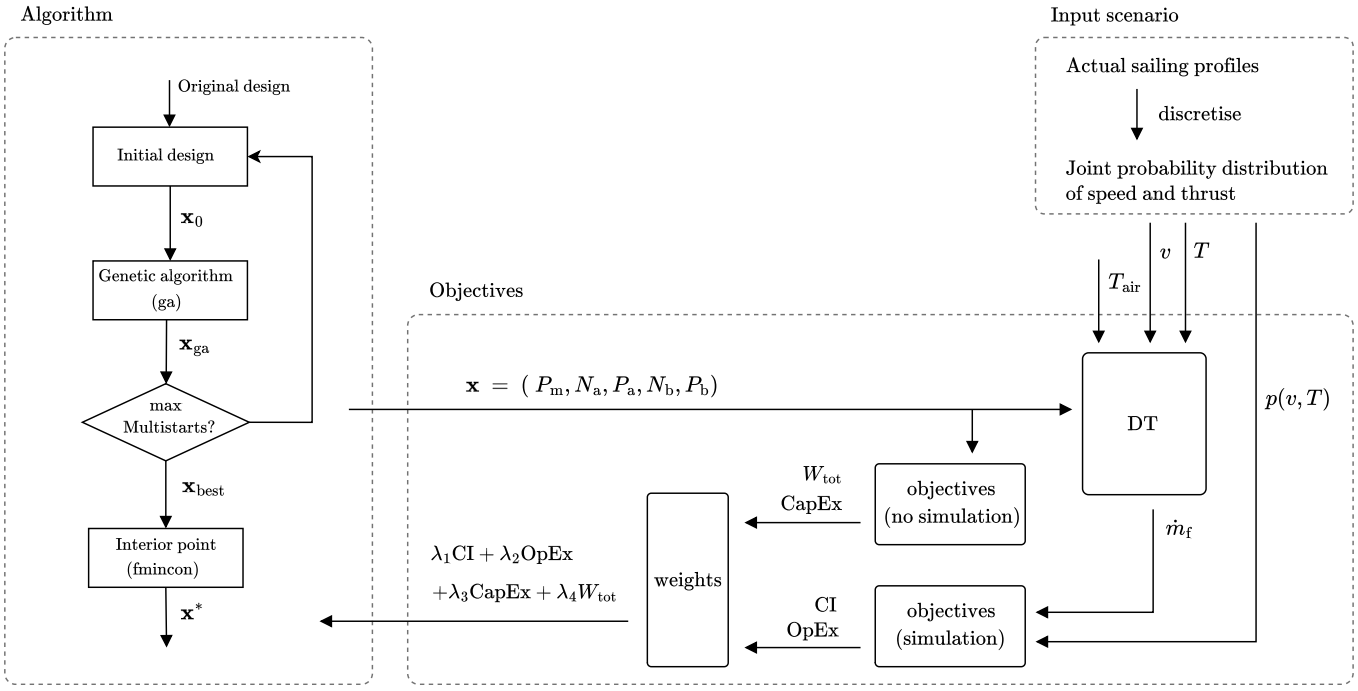

Fig. 9. Description of the multi-objective optimisation framework.

pair $p(v,T)$ and external air temperature T_{air} that defines the hotel load:

$$\mathcal{I} = \{\mathbf{i}_1, \mathbf{i}_2, \mathbf{i}_3, \ldots\}, \quad \mathbf{i}_i = \left(v,\ T,\ p(v,T),\ T_{air}\right). \tag{7}$$

The optimisation problem is subject to a number of boundary constraints (see Table 5):

$$P_m^l \le P_m \le P_m^u, \tag{8}$$
$$N_a^l \le N_a \le N_a^u, \tag{9}$$
$$P_a^l \le P_a \le P_a^u, \tag{10}$$
$$N_b^l \le N_b \le N_b^u, \tag{11}$$
$$P_b^l \le P_b \le P_b^u, \tag{12}$$
$$N_a + N_b \le 5. \tag{13}$$

Diesel generators power range lies between the smallest available engine provided by the manufacturers and engines that do not exceed the height of the main diesel engines by more than 50 %. Finally, the number of diesel generators of type a, type b, and the total number of them is bounded based on the common practice in similar vessel type designs to comply with weight, space and maintenance spare parts limitations.

One technical constraint ensures that sufficient electrical power is installed:

$$N_a\ P_a + N_b\ P_b \ge \left(\frac{2\ P_m}{\eta_m} + \max P_{hotel}\right)\frac{1}{L_{max}}, \tag{14}$$

where maximum electrical hotel power under typical operation is set at 710 kW, the maximum running load of the diesel generators L_{max} is equal to 0.85 and the nominal efficiency of the motors η_m is equal to 0.934.

Table 5
Design variables and lower/upper bounds.

Lower bound		Upper bound		Unit
Symbol	Value	Symbol	Value	
P_m^l	200	P_m^u	5 500	[kW]
N_a^l	1	N_a^u	5	[-]
P_a^l	700	P_a^u	4 529	[kW]
N_b^l	0	N_b^u	4	[-]
P_b^l	700	P_b^u	4 529	[kW]

Another technical constraint prevents the installation of unnecessary diesel generators:

$$N_a\ P_a\ +\left(N_b\ -1\right)\ P_b\ \le\ \left(\frac{2\ P_m}{\eta_m}+\max P_{hotel}\right)\frac{1}{L_{max}}\ , \tag{15}$$

or in the case of $N_b = 0$:

$$\left(N_a-1\right)\ P_a\ \le\ \left(\frac{2\ P_m}{\eta_m}+\max P_{hotel}\right)\frac{1}{L_{max}}\ . \tag{16}$$

Furthermore, there is a redundancy constraint as the maximum hotel load needs to be served by a single diesel generator, hence:

$$P_a,\ P_b \ge \frac{\max P_{hotel}}{L_{max}}\ . \tag{17}$$

3.3. Objective functions

3.3.1. Carbon intensity

In this work, CI is evaluated as the fraction of carbon dioxide emissions M_{CO2} and covered distance Δs over the examined period Δt:

$$\mathrm{CI}\ =\ \frac{M_{CO2}}{\Delta s} \tag{18}$$

Carbon dioxide emissions for a specified optimisation scenario $\mathcal{I}$ are evaluated as a double integral of speed v and thrust T:

$$M_{CO2}=\int_{v}\int_{T}\dot{m}_f(v,T)\ f_{CO2}\ p(v,T)\ \Delta t\ \ dv\,dT\ , \tag{19}$$

where $p(v,T)$ is the probability of occurence of a pair (v,T) following the discretisation of the probability density function as described in [70], f_{CO2} is the carbon coefficient equal to 3.206 as in the calculation of EEDI, and $\dot{m}_f$ is the total fuel consumption for a certain vessel speed v, propeller thrust T, and ambient temperature T_{air}. The covered distance is calculated in a similar manner as:

$$\Delta s\ =\ \int_{v}\int_{T} v\ p(v,T)\ \Delta t\ dv\,dT\ . \tag{20}$$

Fuel consumption of diesel generators and electrical motors of different sizes is simulated using the nominal specific fuel consumption values in Fig. 6 and the normalised part load behaviour described in Figs. 10 and 11.

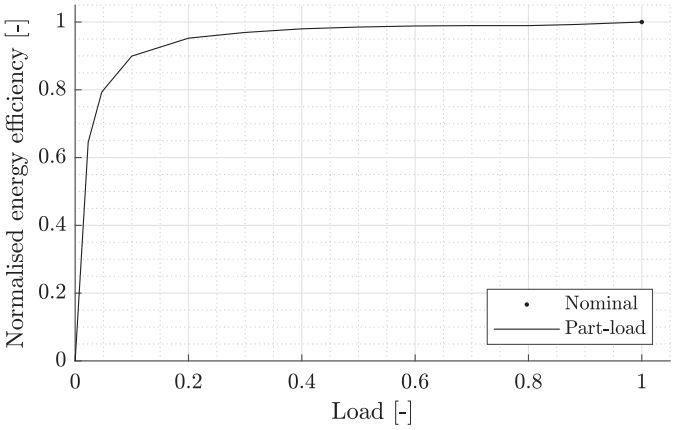

Fig. 10. Normalised energy efficiency of the electrical motors [71].

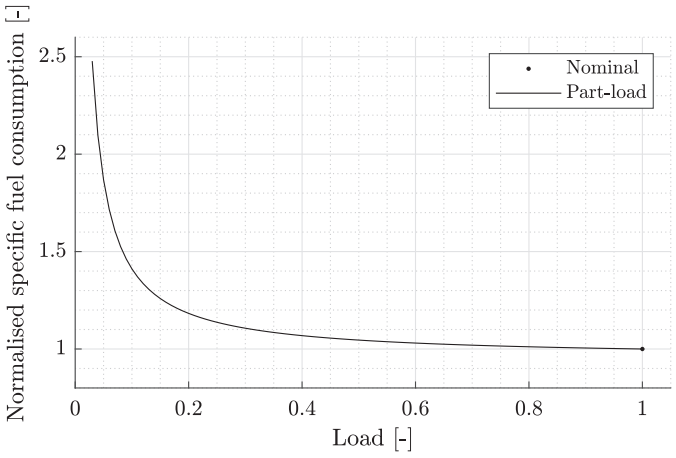

Fig. 11. Normalised specific fuel consumption of the diesel generators.

Table 6
Inflation rate i_f, market interest i_m and years under consideration N_y in this study and examples in literature.

	i_m	i_f	N_y
Livanos et al. [36]	10 %	–	20
Sakalis and Frangopoulos [26]	8 %	3 %	–
Trivyza et al. [18]	7 %	–	25
This study	8 %	3 %	25

3.3.2. Operational expenditure

Net present value of the operational expenditure C_{opex} is evaluated from the yearly amount $C_{opex,y}$:

$$C_{opex}\ =\ \sum_{y=1}^{N_y} C_{opex,y}\left(\frac{1+i_f}{1+i_m}\right)^{y}\ , \tag{21}$$

accounting for inflation rate i_f, market interest rate i_m and years in consideration N_y. Example values from literature and the selection of this study can be found in Table 6. Operational expenditure in a certain year consists mainly of the fuel C_{fuel} and maintenance C_{maint} cost.

$$C_{opex,y}\ =\ C_{maint}+C_{fuel}\ , \tag{22}$$

Fuel cost is given from:

$$C_{fuel}\ =\ \left(M_{f,g}\ +M_{f,e}\right)\ c_f\ , \tag{23}$$

where

$$M_{f,e}\ =\ \int_{v}\int_{T}\dot{m}_{f,e}(v,T)\ p(v,T)\ \Delta t\ dv\,dT\ , \tag{24}$$

$$M_{f,g}\ =\ \int_{v}\int_{T}\dot{m}_{f,g}(v,T)\ p(v,T)\ \Delta t\ dv\,dT\ , \tag{25}$$

is the total fuel mass consumed by the main diesel engines and diesel generators respectively. The fuel price for marine diesel oil was selected at 630 €/ton [26]. The maintenance cost C_{maint} is calculated from the maintenance cost of the main diesel engines $C_{maint,e}$, the diesel generators $C_{maint,g}$, and the electrical motors $C_{maint,m}$:

$$C_{maint}\ =\ C_{maint,e}\ +C_{maint,g}\ +C_{maint,m}\ , \tag{26}$$

$$C_{maint,e}\ =\ \int_{v}\int_{T}2\ P_e\ c_{\mu,e}\ p(v,T)\ \Delta t\ dv\,dT\ , \tag{27}$$

$$C_{maint,g}\ =\ \int_{v}\int_{T}\sum P_g\ c_{\mu,g}\ p(v,T)\ \Delta t\ dv\,dT\ , \tag{28}$$

$$C_{maint,m}\ =\ 2\ P_m\ c_{\mu,m}\ , \tag{29}$$

where c_μ are maintenance cost coefficients providing the cost of a running hour per unit rated power. We use a value of 0.015 €/kWh for both diesel main engines and generators as in [30], and 1 % of capital expenditure for the electrical motors [31].

3.3.3. Capital expenditure

Capital expenditure C_{capex} of the main components of the system consists of capital costs of the main diesel engines $C_{\text{capex,e}}$, diesel generators $C_{\text{capex,g}}$, and electrical motors $C_{\text{capex,m}}$:

$$C_{\text{capex,g}} = \sum P_{\text{g}}\, c_{\text{g}}\,, \tag{30}$$

$$C_{\text{capex,e}} = 2\, P_{\text{e}}\, c_{\text{e}}\,, \tag{31}$$

$$C_{\text{capex,m}} = 2\, P_{\text{m}}\, c_{\text{m}}\,. \tag{32}$$

where c_{g}, c_{m}, and c_{e} are the purchase cost coefficients of diesel generators, electrical motors, and main diesel engines, respectively, in euros per unit rated power, at 350, 32, and 250 €/kW [42].

3.3.4. Total weight

The total weight of the main power supply and propulsion components W_{tot} is given by:

$$W_{\text{tot}} = 2\, W_{\text{e}} + 2\, W_{\text{m}} + \sum W_{\text{g}}\,, \tag{33}$$

where W_{g}, W_{m} are the weights of the diesel generators and electrical motors that can be evaluated from Figs. 5 and 7 respectively, and W_{e} is the weight of each main diesel engine which goes to zero in a fully diesel electric configuration:

$$W_{\text{e}} = \begin{cases} 36.1 & P_{\text{m}} \leq 5\,500\,\text{kW} \\ 0.0 & \text{otherwise} \end{cases} \tag{34}$$

3.3.5. Redundancy terms

The solution to the introduced optimisation problem provides the required electrical motors and diesel generators to sufficiently serve the examined operational scenarios. The actual energy system consists of one additional diesel generator, capable of serving the hotel load for redundancy purposes. We need to account for this with the following redundancy parameters on the capital expenditure:

$$C_{\text{capex,red}} = \begin{cases} \min\left(P_{\text{a}},\, P_{\text{b}}\right) c_{\text{g}}, & \min\left(P_{\text{a}},\, P_{\text{b}}\right) \leq P_{\text{g,thr}}\,, \\ 840\, c_{\text{g}}, & \min\left(P_{\text{a}},\, P_{\text{b}}\right) > P_{\text{g,thr}}\,, \end{cases} \tag{35}$$

and total weight:

$$W_{\text{red}} = \begin{cases} \min\left(W_{\text{a}},\, W_{\text{b}}\right), & \min\left(P_{\text{a}},\, P_{\text{b}}\right) \leq P_{\text{g,thr}}\,, \\ 16.7, & \min\left(P_{\text{a}},\, P_{\text{b}}\right) > P_{\text{g,thr}}\,. \end{cases} \tag{36}$$

The distinction below and above the power threshold $P_{\text{g,thr}}$ is used to balance prioritising a larger number of identical diesel generators against unnecessary installed power. In this work it was chosen to be equal to 1 000 kW.

3.3.6. Energy management strategy

The implemented energy management strategy (EMS) consists of two main tasks. The selection of the propulsion mode and the power allocation to the diesel generators. The first task is modelled based on the curves in Fig. 4 and the ability of electrical motors to meet a certain propulsion power requirement. For the load distribution, generator scheduling, and start–stop logic for a certain number of type a and type b diesel generators, the total electrical load is assumed to be split proportionally among all running diesel generators. An additional diesel generator is activated when the running generators reach the maximum load L_{max}, in the specified order shown in the following diesel generators available power vector:

$$\mathbf{P}_{\text{g}} = [\, \underbrace{P_{\text{a}}, P_{\text{a}}, \ldots}_{N_{\text{a}}}\, \underbrace{P_{\text{b}}, P_{\text{b}}, \ldots}_{N_{\text{b}}}] \, L_{\text{max}} \tag{37}$$

The EMS as implemented in our model assumes that the crew follows it strictly. Previous research on the effect of operational decisions on the examined vessels has shown that this is not actually the case [29]. Additional improvements resulting from better power allocation of the diesel generators are expected to bring further energy savings, but are not expected to alter the main conclusions of this work.

3.4. Problem resolution

The multi-objective optimisation problem reported in Eq. (1)-17 can be formulated and solved following a variety of strategies [72]. In this paper, we adopt a formulation of the problem into a single objective framework by converting the multiple objectives into a weighted sum of the normalised objectives, as detailed in [73]:

$$\begin{aligned} \min_{\mathbf{x}} \quad & \lambda_1\, \text{CI}\left(\mathbf{x}, \mathbf{p}, \mathcal{I}\right) + \lambda_2\, C_{\text{opex}}(\mathbf{x}, \mathbf{p}, \mathcal{I}) + \lambda_3\, C_{\text{capex}}(\mathbf{x}, \mathbf{p}) \\ & + \lambda_4\, W_{\text{tot}}(\mathbf{x}, \mathbf{p})\,. \end{aligned} \tag{38}$$

Classical multi-objective theory shows that for any strictly positive vector of λ values where $\lambda_1, \lambda_2, \lambda_3, \lambda_4 \in [0, 1]$ and $\lambda_1 + \lambda_2 + \lambda_3 + \lambda_4 = 1$, a global minimiser of the weighted sum in Eq. (38) is Pareto-optimal. Sweeping λ values therefore recovers a representative Pareto set in a computationally efficient way [73], while letting stakeholders encode preferences directly in λ values. For example, $\lambda_1 \to 1$, means that stakeholders care more about CI than the rest of the objectives and vice versa for $\lambda_1 \to 0$.

3.5. Optimisation algorithms

Optimisation problems can be classified according to a number of criteria. A typical distinction is between constrained and unconstrained problems based on the presence or absence of linear or non-linear equality or inequality relations among decision variables and between linear and non-linear problems based on the linearity of the objective function or functions. Another important aspect is whether decision variables are real or integer. Many of the mathematical optimisation algorithms discussed in the following paragraphs were originally developed for the case of real variables, making the solution of integer programming problems challenging [74]. Other classes of problems include deterministic and stochastic programming, separable, single or multi-objective programming, and finally, static, dynamic, and intertemporal static programming based on the way they handle time.

Solving algorithms in most textbooks fall into three main categories: search methods, calculus (gradient-based) methods, and stochastic or evolutionary methods [11,75–77]. Search methods and evolutionary methods do not guarantee global optimality of the resulting solutions. Optimisation problems that seek the optimal value of decision variables over time usually use calculus of variations methods or if they include sequences of decisions, dynamic programming methods. In cases where there is no time dependency and discretisation, these problems are turned into multiple static optimisation problems. The solvers used depend on the nature of the examined problem.

Search methods or region elimination methods do not require the objective function to be continuous, they are also suitable in the case of discrete variables, it is sufficient though the functions to be unimodal [76]. The main philosophy behind these methods is the comparison of the objective function value at two different points. In the case of single variable functions, example methods are the Swann method and golden section search. In the case of multi-variable functions, example methods are the univariate method, simplex method and its improved

version by the Nelder and Mead method, Hook and Jeeves method and its improved version by the Rosenbrock method, and Powell method.

Calculus (gradient) methods impose additional requirements on the objective function, as it needs to be unimodal, continuous and differentiable. Example methods in the single variable function case are Newton-Raphson method, Bisection method, and Secant method, while a well known method in the case of multi-variable functions is the generalised reduced gradient method. A special category that uses the benefits of gradient methods is the polynomial approximation methods, with sequential linear and quadratic programming methods (SLP & SQP) being two widely used examples.

A distinct class of algorithms simulates biological, molecular, neurological phenomena, and social metaphors [78]. Examples include genetic and evolutionary algorithms, simulated annealing, and particle swarm optimisation, among others. Genetic algorithms are primarily used because of the nature of ship energy systems optimisation problems [11]:

- no analytical description of objective functions is often the case
- non-continuous objective functions or first-derivative functions
- integer decision variables

3.6. Selected algorithm

The introduced multi-objective optimisation problem of Eqs. (1)-17 has nonlinear and non-convex objective functions and a series of nonlinear constraints. Taking into account the integer nature of some of the decision variables in Eq. (5), the introduced problem can be classified as a Mixed-Integer Nonlinear Programming (MINLP) problem. In order to solve it, different approaches can be exploited [79]. In fact, a series of no-free-lunch theorems [80] ensures that there is no way to choose a priori the best optimisation algorithms for a particular problem.

Recognising the challenges, heuristic approaches such as Genetic Algorithms (GA) can be considered viable solution strategies, as reported in the relevant literature [73,76]. These may not guarantee absolute optimality, but they have demonstrated prowess in delivering high-quality solutions within restricted time frames [76]. However, with heuristic methods, the effective management of constraints is important, and penalty methods must be used to ensure that constraints are respected [81]. Since the convergence of all these algorithms is influenced by the starting point, multi-start strategies are followed [82].

In this study, a hybrid approach is used for the solution of the weighted sum problem of normalised objectives in Eq. (38). As demonstrated in Fig. 9, the first step employs a genetic algorithm utilising the ga function of the Matlab 2022 a[1] environment within a multi-start loop. Table 7 summarises the parameter settings of the GA. As starting points, this methodology uses: (i) the original system configuration and sizing (ii) 100 in the case of single optimisation and 50 in the case of multi-objective optimisation, random points uniformly distributed in the domain induced by the constraints of Eq. 8-17. The GA provides robust global exploration across the discrete–continuous design space, which is crucial for (a) integer variables and (b) non-convexities. Once the GA produces feasible elites, an interior-point method acts as a continuous local optimiser on (P_m, P_a, P_b) conditional on the integer tuple (N_a, N_b). This division of labour matches theory and practice: stochastic search to cross discontinuities/combinatorics; barrier-based Newton methods to exploit local smoothness for fast convergence and tight feasibility. Empirically, this hybridisation reduces variance across runs and improves constraint satisfaction without the heavy penalty tuning required by pure evolutionary schemes.

Table 7
Tuning parameters of the selected optimisation algorithm.

Parameter	Value(s)
Population size	300
Elite count	250
Crossover fraction	0.7
Crossover function	*crossoverscattered*
Max generations to stall	30
Function tolerance	1e-4
Constraint tolerance	1e-4
UseParallel	*true*

[1] https://www.mathworks.com/

Table 8
Optimisation scenarios.

	$v,\ T,\ p(v,T)$	T_{air} [°C]	P_{hotel} [kW]
Calm	Figs. A1 & A2	25.0	605
Calm +25 %	Figs. A1 & A2	25.0	605
Design	Figs. A1 & A2	25.0	605
Vessel 1	Fig. 12(a)	23.4	600
Vessel 2	Fig. 12(b)	22.3	590
Vessel 3	Fig. 12(c)	20.8	585

This algorithm was selected over alternatives such as the NSGA-II, branch-and-bound, or surrogate-assisted frameworks. NSGA-II (and related multi-objective EAs) is powerful for continuous multi-objective problems [83]. In our MINLP setting it requires (a) specialised integer variation/repair operators and (b) non-trivial constraint handling. Maintaining population diversity across multiple objectives and discrete layouts typically increases the number of evaluations. In contrast, the weighted sum approach naturally parallelises over a grid of λ values (independent jobs), and each job benefits from deterministic local refinement to quickly obtain feasible, high-quality points. Mixed-integer branch-and-bound (B&B) and outer-approximation variants are strongest when convex relaxations provide tight bounds. The examined ship energy system models yield non-convex response surfaces; relaxations are weak and node counts escalate rapidly, leading to poor scalability [74]. Finally, a surrogate-assisted optimiser would attempt to build a global surrogate of the entire multi-objective MINLP, trained on a large pre-computed dataset, and then use that surrogate to replace or accelerate optimisation runs. Although powerful in contexts such as CFD-based hull optimisation [84], this approach requires extensive pre-training data, suffers from difficulties in representing mixed-integer discontinuities, and is less transparent for decision support.

3.7. Optimisation scenarios

The design-by-optimisation methodology described in this paper uses probability distributions of actual sailing profiles to account for operational and environmental variability. A complete optimisation scenario in the context of this work $\mathcal{I}$ consists of a set of tuples of vessel speed v, thrust T, the probability of occurrence of each pair $p(v,T)$ following discretisation [70], and the external air temperature T_{air} that corresponds to a specific electrical hotel load as seen in Table 8. In this work, the sailing profiles of three sister vessels are used, although this methodology can also utilise the profiles of vessels serving similar missions. Fig. 12 provides the discretised joint probability distributions of the three OPVs.

Optimisation over actual joint probability distributions is also compared to optimisation over simpler scenarios commonly considered in the concept design phase. EEDI is not one of these scenarios as it remains unchanged for the different design options. These scenarios use typical speed profiles for the type of considered vessel and a number of ship resistance curves. In this application, a calm water resistance curve based on scale-model towing-tank tests, a fixed 25 % increase in calm water resistance, and a design resistance curve that is the result of seakeeping tank tests under certain environmental conditions are used. In order to enhance readability, the used OPV speed profile and the three resistance curves are provided in a separate appendix.

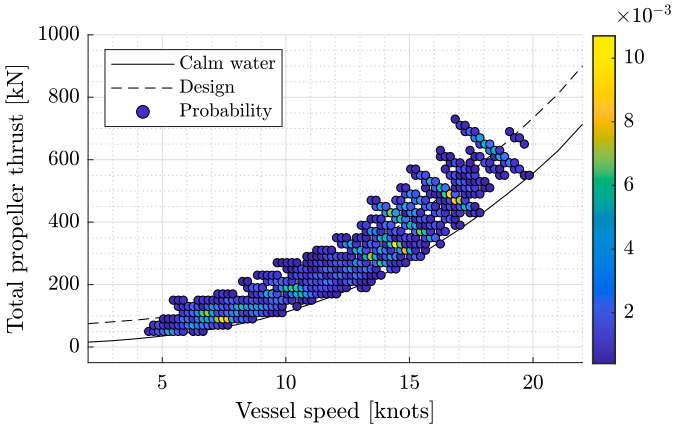

(a) Vessel 1

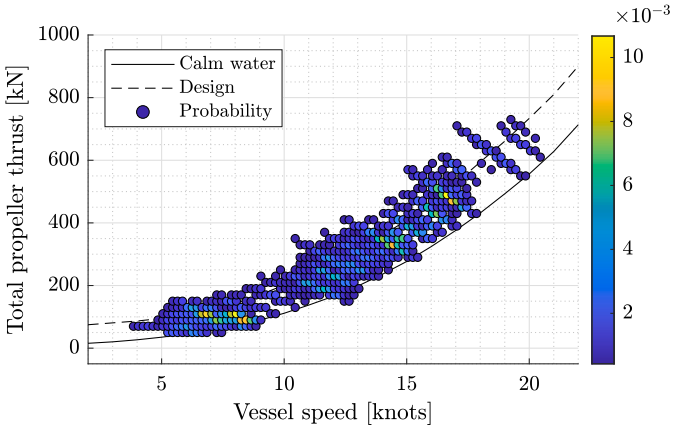

(b) Vessel 2

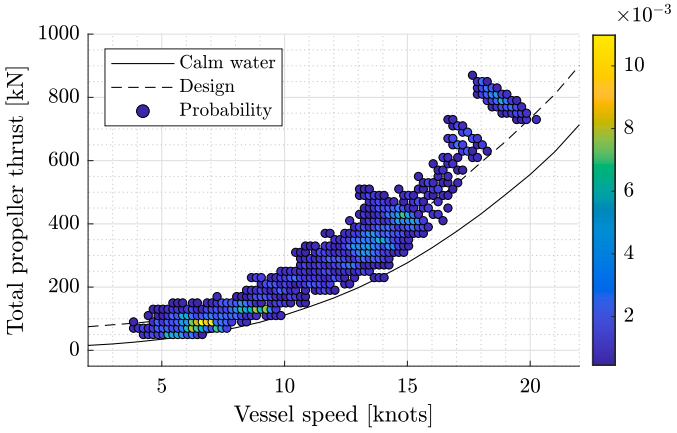

(c) Vessel 3

Fig. 12. Discretised joint probability distribution of vessel speed and thrust in the case of the three sister OPV vessels.

Finally, Table 8 provides guidelines for the information used in the different scenarios. The time spent at sea was assumed to be 20 % of a calendar year (see Table 3).

4. Results

4.1. Single-objective optimisation

This section discusses the results of the four single-objective optimisation problems described by Eq. (1)-4. The results of these problems are useful to understand the individual influence of each objective on the optimal design of the examined system. Being simpler than the multi-objective problem, they make it possible to identify the influence of the different optimisation scenarios on the optimal solutions as well. Mathematically, these problems derive from Eq. (38) by setting the weight of the objective i in question equal to one ($\lambda_i = 1$), and all the weights of the rest of the objectives equal to zero ($\lambda_j = 0,\ \forall j \neq i$), where $i, j \in \{1, 2, 3, 4\}$. Carbon intensity and operational expenditure required the simulation of the energy system's operation over the examined operating scenarios, while total weight and capital expenditure were just calculated over different feasible solutions. The original design mentioned in the results refers to the original size of electrical motors, diesel generators, and manufacturers, though with a single reduction stage gearbox rather than two on electrical mode. Table 9 provides the values of the objective functions for the original design.

Table 9
Values of the objective functions for the benchmark original design.

Input		Decision variables		Objectives	
	pto [-]	P_m [kW]	P_{gen} [kW]	CI [kgCO2/nm]	OPEX [x10^3 €]
Calm	no	2x 400	2x 910	179.7	–
Calm +25 %	no	2x 400	2x 910	210.8	16 853
Design	no	2x 400	2x 910	236.0	18 724
Vessel 1	no	2x 400	2x 910	203.7	14 610
Vessel 2	no	2x 400	2x 910	199.0	13 761
Vessel 3	no	2x 400	2x 910	215.0	13 189
				CAPEX [x10^3 €]	W_{tot} [tons]
-	no	2x 400	2x 910	3 681	116.5

The result of the carbon intensity minimisation problem is mainly driven by the nominal specific fuel consumption curve of the examined diesel generators which can be found in Fig. 6. Table 10 provides the results for the carbon intensity optimisation problem in the case of calm water conditions, with or without a 25 % sea margin, design conditions, and the sailing profiles of the three vessels of the examined class. The size of diesel generators that mostly appears in different solutions is 1 870 or 3 230 kW. Slightly smaller diesel generators have a worse nominal specific fuel consumption, and slightly larger ones operate at a lower load for the same specific fuel consumption, which according to Fig. 11 indicates an overall higher fuel consumption. The size of the electrical motors is driven by the fuel efficiency of the diesel generators. Carbon intensity is proportionally related to fuel consumption; hence, the result is one large engine compared to multiple small ones.

Operational expenditure consists of the cost of fuel and maintenance. The assumption in this work is that the maintenance cost in €/hour depends on the nominal power of the engine. According to this assumption, running smaller and less expensive per hour diesel generators is better than running larger engines. The same applies to running on electrical propulsion instead of main diesel engines at lower speeds, as their maintenance cost per running hour is higher, proportional to the rated power. Table 11 provides the results of the operational expenditure minimisation problem. Savings of the order of one million euros in net present value are established in all scenarios. Again, calm water with sea margin and design conditions overestimate savings, as well as the height of operational expenditure over a 25-year horizon.

The solution to the optimisation problem is trivial in the case of capital expenditure and the total weight of the energy system. This happens because the increase in the size of electrical motors is not offset by a decrease in the size of main diesel engines. Therefore, the optimal solution is the smallest electrical propulsion plant.

A general observation on the results of both the CI and OPEX problems is that the different optimisation scenarios influence the optimal system topology and sizing. Calm water conditions, which are the main consideration in EEDI calculations, even result in a misleading overestimation of energy savings. Finally, as seen in Table 12, the design

Table 10
Single-objective CI minimisation problem results, with and without power take-off, including the percentage improvement to the original benchmark case.

Input		Decision variables					Objective	
	pto [-]	P_m [kW]	N_a [-]	P_a [kW]	N_b [-]	P_b [kW]		CI [kgCO2/mile]
Calm	no	2x 1 420	1x	3 245	2x	895	(−3.5 %)	173.3
Calm +25 %	no	2x 1 700	1x	3 230	3x	880	(−2.7 %)	205.2
Design	no	2x 1 260	1x	840	1x	3 230	(−2.4 %)	230.3
Vessel 1	no	2x 1 350	1x	825	2x	3 230	(−2.9 %)	197.9
Vessel 2	no	2x 1 175	2x	835	1x	3 230	(−2.9 %)	193.2
Vessel 3	no	2x 700	4x	835	–	–	(−2.9 %)	208.8
Calm	yes	2x 1 365	1x	3 230	2x	905	(−4.6 %)	171.4
Calm +25 %	yes	2x 1 275	1x	3 230	1x	950	(−3.4 %)	203.6
Design	yes	2x 1 380	1x	3 290	2x	890	(−3.1 %)	228.7
Vessel 1	yes	2x 1 370	1x	3 270	2x	840	(−3.9 %)	195.8
Vessel 2	yes	2x 1 250	1x	3 235	1x	840	(−3.9 %)	191.2
Vessel 3	yes	2x 1 405	1x	3 230	2x	855	(−3.5 %)	207.5

Table 11
Single-objective net present value of OPEX minimisation problem results, with and without power take-off, including the percentage improvement to the original benchmark case.

Input		Decision variables					Objective	
	pto [-]	P_m [kW]	N_a [-]	P_a [kW]	N_b [-]	P_b [kW]		OPEX [x10^3 €]
Calm	no	2x 1 820	3x	1 000	2x	1 230	(−10.9 %)	13 118
Calm +25 %	no	2x 1 770	2x	835	3x	1 210	(−9.1 %)	15 323
Design	no	2x 2 125	3x	835	2x	1 870	(−8.2 %)	17 181
Vessel 1	no	2x 2 150	3x	840	2x	1 880	(−9.5 %)	13 229
Vessel 2	no	2x 2 420	2x	1 875	3x	1 070	(−9.2 %)	12 495
Vessel 3	no	2x 2 255	2x	1 875	3x	935	(−9.2 %)	11 983
Calm	yes	2x 1 740	1x	1 900	4x	835	(−12.4 %)	12 894
Calm +25 %	yes	2x 1 800	1x	1 870	4x	880	(−10.0 %)	15 164
Design	yes	2x 2 130	1x	3 255	4x	900	(−9.2 %)	17 008
Vessel 1	yes	2x 2 195	1x	3 230	4x	830	(−11.0 %)	13 004
Vessel 2	yes	2x 2 170	1x	3 235	4x	860	(−10.5 %)	12 317
Vessel 3	yes	2x 2 190	2x	1 870	3x	880	(−9.7 %)	11 908

Table 12
Carbon intensity comparison on the actual profile of Vessel 3 across designs optimised for different scenarios (without power take-off).

Optimised for	Decision variables					Objective
	P_m [kW]	N_a [-]	P_a [kW]	N_b [-]	P_b [kW]	CI [kgCO2/mile]
Calm	2x 1 420	1x	3 245	2x	895	+0.4 %
Calm+25 %	2x 1 700	1x	3 230	3x	880	+0.3 %
Design	2x 1 260	1x	840	1x	3 230	+0.3 %
Actual	2x 700	4x	835	–	–	208.8

consideration of calm water or design conditions results in solutions that can potentially be suboptimal in actual operations.

4.2. Capital expenditure and total weight

Capital expenditure and the total weight of the system are both parameters of significant importance in the design of a system. Especially in the way modelled in this work, they also seem to have an almost linear correlation, as can be seen in Fig. 13. This figure demonstrates one thousand sampled designs, showing an R^2 value of 0.97. This correlation allows us to proceed with one of the two, in this case capital expenditure, set $\lambda_4 = 0$ and report total system weight with our results.

4.3. Multi-objective optimisation

Multi-function ships are complex ships that serve many types of missions. This means that their design unavoidably requires a performance trade-off evaluated with a number of objectives. This section provides the results of the multi-objective optimisation problem and solving strategy introduced in Section 3. The result of the optimisation algorithm is a number of solutions that form the so-called Pareto front. Fig. 14 provides a three-dimensional visual representation of the Pareto front, and Table B1 and Fig. B1 in the appendices provide all details of the solutions

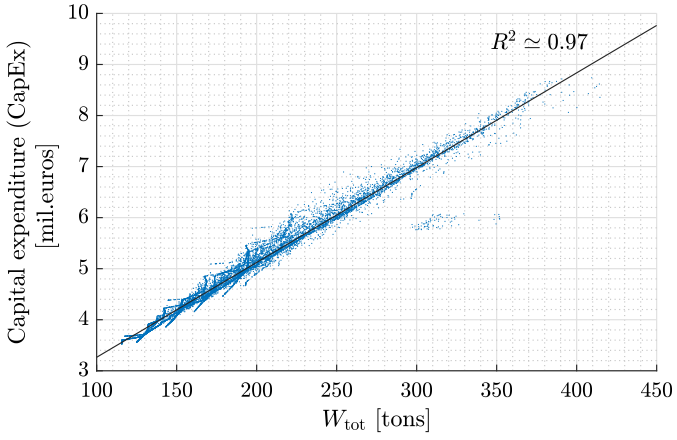

Fig. 13. Linear correlation of capital expenditure (CAPEX) and total weight of the system W_{tot} for 10 000 randomly generated designs.

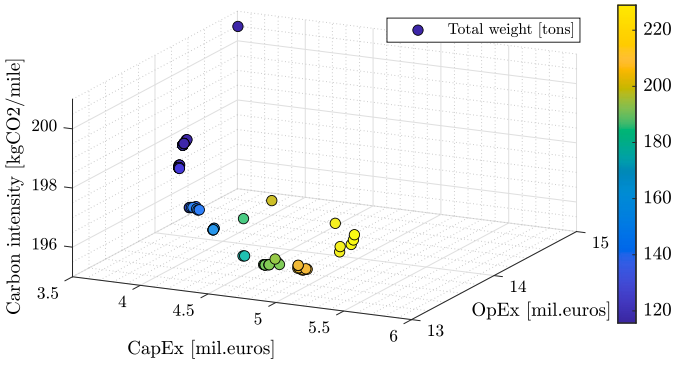

Fig. 14. Multi-dimensional Pareto front.

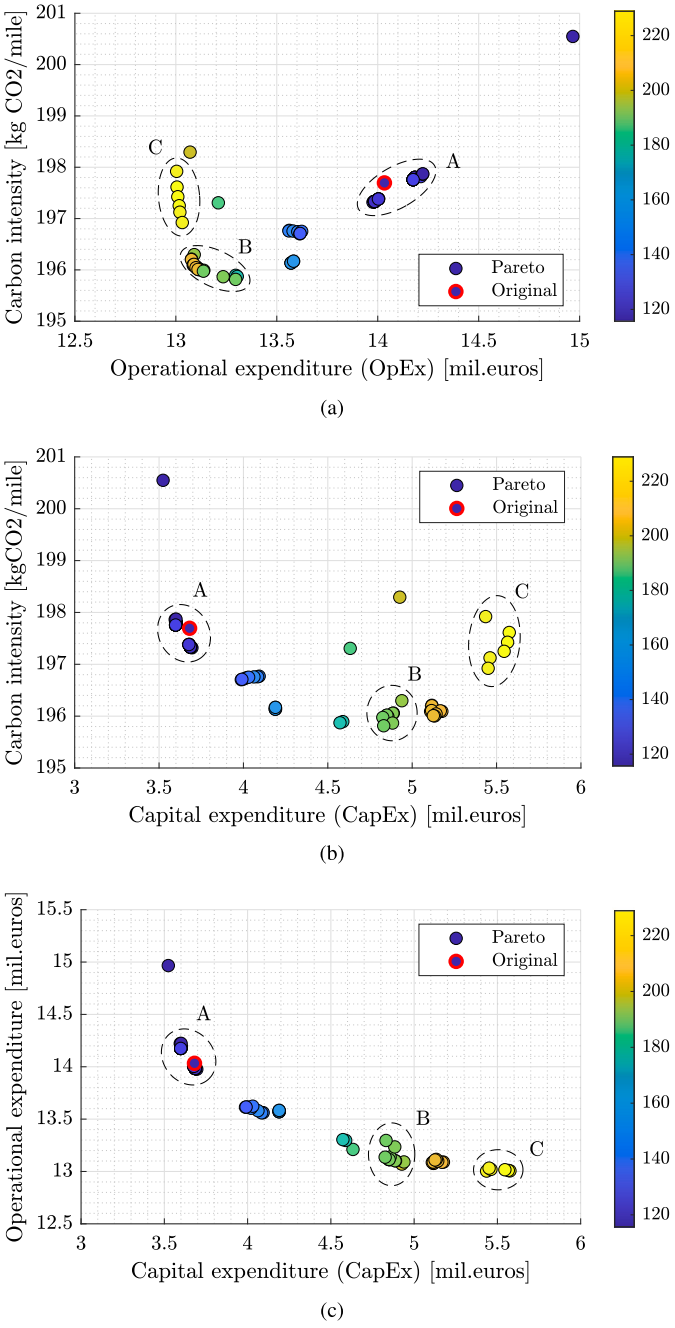

Fig. 15. Two-dimensional views of the Pareto front with solutions coloured based on the total system weight in tons and three different groups of solutions.

to the different prioritisation problems. The input scenario in the case of the multi-objective optimisation problem is the actual sailing profile of vessel 1, and power take-off is included.

Fig. 15 allows for the two-dimensional examination of the Pareto front. A closer look at certain regions which are described in more detail in Table 13 provides additional insight into the behaviour and characteristics of the solutions. In region A, capital expenditure is low, driven by the small size of electrical motors and diesel generators. The system is relatively simple, as only one running diesel generator is necessary. As the size of the electrical system increases at the cost of additional capital costs and weight, both carbon intensity and operational costs improve up to the designs of region B. This is mainly explained by the fact that smaller electrical motors are less expensive to maintain per running hour compared to main diesel engines and because main diesel engines are inefficient at low loads. This region which marks the minimum carbon intensity for our problem corresponds to electrical motors three to four times larger than the original design and three diesel generators in total. An additional increase in the size of the electrical system increases capital costs. Operational costs improve even more, as the larger motors in region C further prevent the main diesel engines from running, lowering maintenance costs. However, the maintenance benefit of the many small diesel generators is overshadowed by their low fuel efficiency. This is a region where the main engines are sufficiently efficient, resulting in poorer carbon intensity performance.

In summary, minimisation of capital expenditure indicates designs near region A. If carbon intensity is prioritised, designs near region B show superior performance. Finally, a compromise can be found between operational expenditure and carbon intensity between regions B and C.

4.4. Sensitivity

The previous paragraph discussed the solution of the multi-objective problem and the formation of the Pareto front. This paper examines the trade-offs and mechanisms behind different objectives and provides the engineering rationale behind the selection of designs from the different Pareto front regions. Many volatile parameters influence the values of the objectives. Typical values reported in various sources are used with deviations expected to increase the dominance of influenced objectives but not change the qualitative characteristics and trade-offs discussed in the previous paragraph. For example, if the purchase prices of electrical motors increase, they will become less attractive as an option, but they will still bring maintenance cost reductions and environmental benefits.

With respect to total capital expenditure, the purchase cost of the main diesel engines and the smallest electrical propulsion system configuration form a fixed cost that determines the minimum capital expenditure of the design solutions. The relative span of the capital expenditure axis is then entirely determined by the cost of larger electrical motors and diesel generators. The type and quality of the fuel, the non-ISO working conditions, and the ageing of the components influence fuel consumption, hence the absolute value of carbon intensity. In the same

Table 13
Average values of design parameters for the different groups of the Pareto front regions.

Group	$\overline{P_m}$ [kW]	N_a [-]	$\overline{P_a}$ [kW]	N_b [-]	$\overline{P_b}$ [kW]
A	420	1	1 900	0	–
B	1 590	1	3 260	2	870
C	2 090	1	3 240	4	880

way, the time horizon for our study, the yearly sailing time, inflation and interest rates directly impact the minimum operational expenditure net present value. Finally, the most important expected influence is the governing fuel prices and maintenance costs per running hour, as these can affect the relative improvement of operational expenditure among the designs in region C compared to region B.

4.5. Computational efficiency

Genetic algorithms are considered computationally demanding algorithms [35]. The results show that each algorithm start requires thousands of fitness function calls. Tables C1 and C2 found in the appendices provide metrics on the computational efficiency of the algorithm in the case of CI and OPEX single-objective optimisation problems and of the multi-objective problem, respectively. The CI problem requires around 30 % fewer calls than the OPEX problem. Fitness function calculation times of more than a couple of seconds and the lack of parallel computing would lead to solving times much higher than a single day for each one of the 83 different problems solved to form the Pareto front. It is also important to note the significant increase in computational time resulting from the use of the actual sailing profiles of the vessels. Despite this challenge, the selected optimisation framework delivered quality results within the limits of computers capable of supporting the parallel running of at least five workers.

5. Conclusions

This paper provides a multi-objective optimisation framework for the early-stage design of ship energy systems from an environmental, financial, and technical perspective. This framework is based on probability distributions of actual sailing profiles of vessels following similar missions and utilises an accurate and computationally inexpensive digital twin approach for the prediction of the ship's operation. It can also be applied in the case of retrofitting existing vessels, although constraints on the dimensions of system components are expected to be stricter. Its potential to reduce carbon emissions, capital and operational costs, and the total weight of systems is demonstrated through the topology selection and sizing of the electrical part of the hybrid propulsion system of a class of ocean patrol vessels.

This methodology can also be applied in the case of different ship types with different power supply and propulsion system architectures. Nevertheless, the ships that benefit the most are those that follow diverse operational profiles and operate under diverse environmental conditions. The specific results for hybrid propulsion can be generalised on multi-function ships that perform a wide range of services at sea, sailing usually at a low and a high speed, such as support vessels, cruise ships, naval vessels, offshore service vessels, wind turbine installation vessels, and crane vessels. Ships utilising one operational-design speed like oil/LNG tankers or bulk carriers can also benefit from this methodology, although the uncertainty of their operation is mainly linked to their loading condition. Finally, the required logging duration of operational data might be lower for case studies with regular schedules such as ferries, however, a minimum logging period of a year is required to include any seasonal effect.

This analysis highlights several key insights into the design and operational trade-offs of hybrid-electric and hybrid propulsion systems for ships. The variability in environmental, financial, and technical performance across different sailing profiles, even within vessels of the same class, underscores the inherent difficulty in identifying a universally optimal design. This variability demonstrates that calm water conditions used by the regulated EEDI or nominal design conditions, often derived by applying a standard sea margin, can lead to misleading performance expectations. Relying solely on such assumptions may result in overestimated energy and financial savings and ultimately suboptimal designs.

A major advantage of the adopted steady-state modelling approach lies in its ability to incorporate joint probability distributions of vessel speed and thrust to characterise realistic operational profiles. This method significantly reduces computational time, thereby enabling the exploration of a much wider design space compared to transient simulations.

From a design perspective, larger electrical motors up to 40 % the size of the main diesel engines improve the carbon intensity and operational expenditure. However, the sizing strategy for diesel generators is not the same when prioritising each objective. Few large diesel generators improve carbon intensity while more smaller ones improve operational costs, mainly because of the lower maintenance costs per running hour. Their size is driven by specific fuel consumption jumps in market catalogues linked to shifts in bore size of different families of engines. Furthermore, power take-off (PTO) improved both carbon intensity and operational expenditure in almost all examined cases. Interestingly enough, its presence appeared to balance the effect of diverse operational and environmental conditions as well.

Finally, from a capital expenditure perspective that is mainly driven by the size of electrical motors, increasing capital investment appears to improve both carbon intensity and life-cycle operational expenditure. However, there exists a limit point defined by direct comparison of the fuel efficiency of mechanical and electrical propulsion after which carbon intensity increases again even if the maintenance cost of electrical motors and diesel generators is lower than that of the main diesel engines.

Future work could focus on a number of directions. For instance, the comparison of the weighted sum hybrid approach in the solution of the multi-objective problem to algorithms such as NSGA-II and multi-objective particle swarm optimisation (MOPSO). Alternative problem formulations to the MINLP formulation could allow the employment of computationally more efficient gradient or search optimisation algorithms. A different selection of design space with a selection from a set of actual diesel generators and motors would result in a multi-objective combinatorial optimisation problem (MOCO). The recommended modelling approach could also be used in optimisation problems that consider hybrid power supply, with the use of batteries and fuel cells, or in two-stage topology/sizing and enhanced EMS optimisation methodologies, although battery charging and discharging phases require a creative way to handle time dependence. Finally, the use of actual sailing profiles that quantify the scattering of operating conditions, as demonstrated in this paper, could be integrated into robust design optimisation problems or in the design of robust controllers.

CRediT authorship contribution statement

Nikolaos Vasilikis: Writing – original draft, Visualization, Software, Methodology, Data curation, Conceptualization. **Rinze Geertsma:** Writing – review & editing, Supervision, Conceptualization. **Andrea Coraddu:** Writing – review & editing, Supervision, Methodology, Conceptualization.

Declaration of competing interest

The authors declare that they have no known competing financial interests or personal relationships that could have appeared to influence the work reported in this paper.

Acknowledgements

This work is supported by The Netherlands Organisation for Scientific Research (NWO) [Nederlandse Organisatie voor Wetenschappelijk Onderzoek] project 'AssetDrive: Translating maintenance analysis and operational data to enhanced ship system design and performance contracts' (ALWTW.016.042). Moreover, this work utilised the increased computing capabilities of the Delft Supercomputer (Phase 1) [85].

Appendix A

This appendix provides a typical vessel speed profile for an OPV and the resistance curves from scale-model towing-tank tests that are used to build the common practice optimisation scenarios.

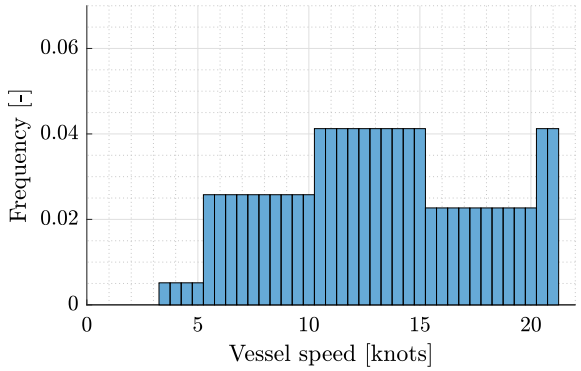

Fig. A1. Typical vessel speed profile for an OPV.

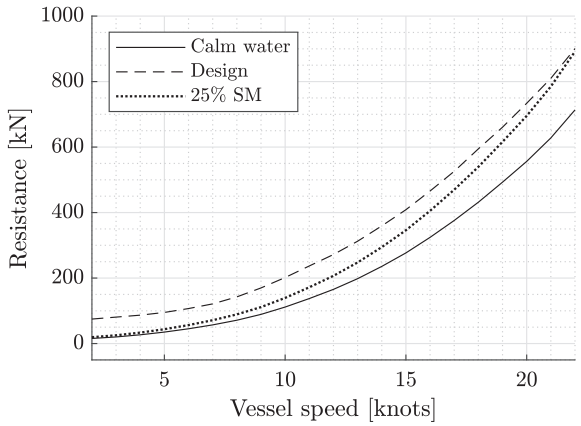

Fig. A2. Resistance curves deriving from scale-model towing-tank tests.

Appendix B

This appendix provides all details of the eighty-three designs that form the Pareto front.

Table B1
Pareto optimal solutions of the multi-objective optimisation problem.

	Weights				Decision variables					Objectives			
	λ_1 [-]	λ_2 [-]	λ_3 [-]	λ_4 [-]	P_m [kW]	N_a [-]	P_a [kW]	N_b [-]	P_b [kW]	CI [kgCO2/mile]	OPEX [x10^3 €]	CAPEX [x10^3 €]	W_{tot} [tons]
-	1.000	0.000	0.000	0.000	1 370	1x	3 270	2x	840	195.8	13 296.1	4 831.2	189
-	0.000	1.000	0.000	0.000	2 195	1x	3 230	4x	830	197.9	13 004.0	5 435.1	225
-	0.000	0.000	1.000	0.000	250	1x	1 468	–	–	200.5	14 966.4	3 523.8	116
1	0.100	0.900	0.000	0.000	2 120	1x	3 235	4x	918	197.6	13 005.9	5 575.2	229
2	0.087	0.783	0.130	0.000	1 720	1x	1 870	4x	835	198.3	13 070.5	4 926.4	201
3	0.071	0.643	0.286	0.000	1 415	1x	1 870	3x	848	197.3	13 210.5	4 632.7	184
4	0.059	0.529	0.412	0.000	747	1x	1 870	1x	857	196.7	13 615.4	4 002.4	148
5	0.040	0.360	0.600	0.000	410	1x	1 877	–	–	197.4	14 003.6	3 677.0	122
6	0.200	0.800	0.000	0.000	2 091	1x	3 234	4x	914	197.4	13 009.7	5 565.4	229
7	0.174	0.696	0.130	0.000	1 740	1x	3 233	2x	1 003	196.3	13 091.0	4 938.7	194
8	0.143	0.571	0.286	0.000	840	1x	1 873	1x	1 114	196.8	13 561.8	4 093.3	146
9	0.118	0.471	0.412	0.000	430	1x	1 924	–	–	197.3	13 976.6	3 694.8	124
10	0.080	0.320	0.600	0.000	410	1x	1 873	–	–	197.4	14 003.2	3 675.8	126

(continues on next page)

Table B1 *(continues from previous page)*

	Weights				Decision variables					Objectives			
	λ_1 [-]	λ_2 [-]	λ_3 [-]	λ_4 [-]	P_m [kW]	N_a [-]	P_a [kW]	N_b [-]	P_b [kW]	CI [kgCO2/mile]	OPEX [x10^3 €]	CAPEX [x10^3 €]	W_{tot} [tons]
11	0.300	0.700	0.000	0.000	2 063	1x	3 236	4x	903	197.3	13 016.7	5 544.9	228
12	0.261	0.609	0.130	0.000	1 663	1x	3 230	2x	906	196.1	13 102.1	4 888.2	192
13	0.214	0.500	0.286	0.000	840	1x	1 873	1x	1 089	196.8	13 560.0	4 084.3	146
14	0.176	0.412	0.412	0.000	420	1x	1 898	–	–	197.3	13 983.9	3 685.3	120
15	0.120	0.280	0.600	0.000	330	2x	835	–	–	197.8	14 175.3	3 598.2	126
16	0.350	0.650	0.000	0.000	2 041	1x	3 232	4x	857	197.1	13 020.1	5 461.2	226
17	0.304	0.565	0.130	0.000	1 640	1x	3 260	2x	863	196.0	13 112.7	4 851.9	190
18	0.250	0.464	0.286	0.000	817	1x	1 870	1x	1 033	196.8	13 580.6	4 062.2	149
19	0.206	0.382	0.412	0.000	420	1x	1 899	–	–	197.3	13 984.0	3 685.6	120
20	0.140	0.260	0.600	0.000	330	1x	1 675	–	–	197.8	14 183.6	3 601.5	116
21	0.400	0.600	0.000	0.000	1 999	1x	3 231	4x	852	196.9	13 031.9	5 450.1	225
22	0.348	0.522	0.130	0.000	1 642	1x	3 276	2x	858	196.0	13 113.7	4 853.0	190
23	0.286	0.429	0.286	0.000	770	1x	1 962	1x	835	196.7	13 604.0	4 020.6	147
24	0.235	0.353	0.412	0.000	420	1x	1 899	–	–	197.3	13 984.0	3 685.6	120
25	0.160	0.240	0.600	0.000	330	2x	835	–	–	197.8	14 175.3	3 598.2	126
26	0.450	0.550	0.000	0.000	1 747	1x	3 231	3x	839	196.2	13 077.8	5 116.7	207
27	0.391	0.478	0.130	0.000	1 661	1x	3 234	2x	902	196.1	13 102.3	4 885.4	192
28	0.321	0.393	0.286	0.000	740	1x	1 926	1x	871	196.8	13 623.2	4 030.8	143
29	0.265	0.324	0.412	0.000	420	1x	1 898	–	–	197.3	13 983.9	3 685.3	120
30	0.180	0.220	0.600	0.000	330	2x	835	–	–	197.8	14 175.3	3 598.2	126
31	0.500	0.500	0.000	0.000	1 743	1x	3 230	3x	839	196.2	13 077.2	5 116.3	207
32	0.435	0.435	0.130	0.000	1 640	1x	3 288	2x	849	196.0	13 115.3	4 846.7	190
33	0.357	0.357	0.286	0.000	740	1x	1 872	1x	835	196.7	13 613.9	3 987.4	145
34	0.294	0.294	0.412	0.000	420	1x	1 899	–	–	197.3	13 984.0	3 685.5	120
35	0.200	0.200	0.600	0.000	330	2x	835	–	–	197.8	14 175.3	3 598.2	126
36	0.550	0.450	0.000	0.000	1 701	1x	3 262	3x	875	196.1	13 089.5	5 175.8	208
37	0.478	0.391	0.130	0.000	1 610	1x	3 264	2x	867	196.0	13 138.5	4 855.9	190
38	0.393	0.321	0.286	0.000	740	1x	1 882	1x	835	196.7	13 615.4	3 990.9	136
39	0.324	0.265	0.412	0.000	420	1x	1 899	–	–	197.3	13 984.0	3 685.5	120
40	0.220	0.180	0.600	0.000	330	1x	1 674	–	–	197.8	14 183.5	3 601.1	116
41	0.600	0.400	0.000	0.000	1 701	1x	3 231	3x	835	196.1	13 086.0	5 109.2	207
42	0.522	0.348	0.130	0.000	1 640	1x	3 270	2x	857	196.0	13 114.6	4 849.8	190
43	0.429	0.286	0.286	0.000	420	1x	1 899	–	–	197.3	13 984.0	3 685.6	120
44	0.353	0.235	0.412	0.000	420	1x	1 899	–	–	197.3	13 984.0	3 685.6	120
45	0.240	0.160	0.600	0.000	330	1x	1 672	–	–	197.8	14 183.2	3 600.3	116
46	0.650	0.350	0.000	0.000	1 700	1x	3 236	3x	875	196.1	13 088.0	5 166.7	208
47	0.565	0.304	0.130	0.000	1 370	1x	3 271	1x	1 035	195.9	13 296.3	4 588.9	174
48	0.464	0.250	0.286	0.000	420	1x	1 900	–	–	197.3	13 984.1	3 685.8	120
49	0.382	0.206	0.412	0.000	420	1x	1 899	–	–	197.3	13 984.1	3 685.7	120
50	0.260	0.140	0.600	0.000	330	2x	835	–	–	197.8	14 175.3	3 598.2	126
51	0.700	0.300	0.000	0.000	1 702	1x	3 245	3x	836	196.1	13 089.6	5 114.9	207
52	0.609	0.261	0.130	0.000	1 350	1x	3 259	1x	1 004	195.9	13 304.2	4 572.2	174
53	0.500	0.214	0.286	0.000	420	1x	1 900	–	–	197.3	13 984.1	3 685.7	120
54	0.412	0.176	0.412	0.000	410	1x	1 883	–	–	197.4	14 004.3	3 679.3	118
55	0.280	0.120	0.600	0.000	330	2x	835	–	–	197.8	14 175.3	3 598.2	126
56	0.750	0.250	0.000	0.000	1 664	1x	3 230	3x	860	196.0	13 099.9	5 141.6	207
57	0.652	0.217	0.130	0.000	950	1x	3 245	–	–	196.1	13 571.6	4 190.6	153
58	0.536	0.179	0.286	0.000	420	1x	1 906	–	–	197.3	13 984.9	3 688.2	121
59	0.441	0.147	0.412	0.000	330	2x	835	–	–	197.8	14 175.3	3 598.3	126
60	0.300	0.100	0.600	0.000	330	1x	1 674	–	–	197.8	14 183.4	3 601.0	116
61	0.800	0.200	0.000	0.000	1 640	1x	3 298	3x	838	196.0	13 115.5	5 132.9	206
62	0.696	0.174	0.130	0.000	950	1x	3 241	–	–	196.1	13 570.7	4 189.0	153
63	0.571	0.143	0.286	0.000	420	1x	1 900	–	–	197.3	13 984.1	3 685.8	120
64	0.471	0.118	0.412	0.000	330	1x	1 675	–	–	197.8	14 183.6	3 601.5	116
65	0.320	0.080	0.600	0.000	330	2x	835	–	–	197.8	14 175.3	3 598.2	126
66	0.850	0.150	0.000	0.000	1 640	1x	3 239	3x	848	196.0	13 109.8	5 125.4	207
67	0.739	0.130	0.130	0.000	940	1x	3 243	–	–	196.2	13 582.8	4 189.3	153
68	0.607	0.107	0.286	0.000	420	1x	1 899	–	–	197.3	13 984.0	3 685.6	120
69	0.500	0.088	0.412	0.000	330	1x	1 677	–	–	197.8	14 183.7	3 602.0	116
70	0.340	0.060	0.600	0.000	330	2x	835	–	–	197.8	14 175.3	3 598.2	126
71	0.900	0.100	0.000	0.000	1 613	1x	3 272	2x	836	196.0	13 136.6	4 825.9	189
72	0.783	0.087	0.130	0.000	950	1x	3 239	–	–	196.1	13 570.4	4 188.6	153
73	0.643	0.071	0.286	0.000	420	1x	1 900	–	–	197.3	13 984.1	3 685.9	120
74	0.529	0.059	0.412	0.000	325	2x	835	–	–	197.8	14 213.1	3 597.9	126
75	0.360	0.040	0.600	0.000	325	1x	1 660	–	–	197.9	14 222.0	3 595.7	116
76	0.950	0.050	0.000	0.000	1 450	1x	3 259	2x	905	195.9	13 234.4	4 883.6	191
77	0.826	0.043	0.130	0.000	940	1x	3 244	–	–	196.2	13 583.0	4 189.6	153
78	0.679	0.036	0.286	0.000	410	1x	1 875	–	–	197.4	14 003.4	3 676.6	123
79	0.559	0.029	0.412	0.000	325	1x	1 673	–	–	197.9	14 223.2	3 600.4	116
80	0.380	0.020	0.600	0.000	330	2x	835	–	–	197.8	14 175.3	3 598.2	126

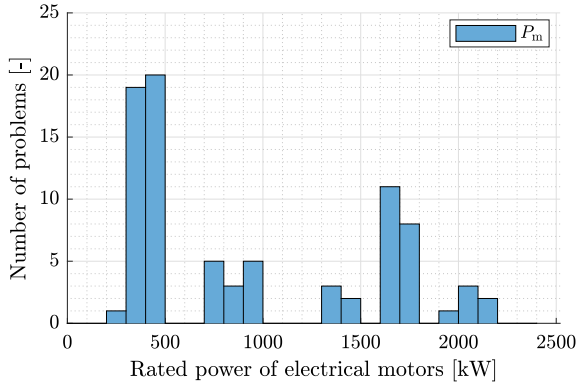

(a)

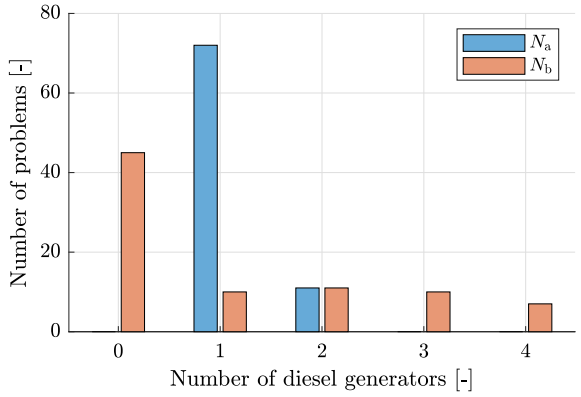

(b)

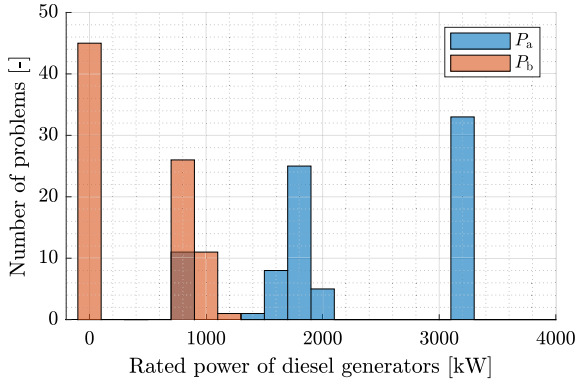

(c)

Fig. B1. Histograms of the solution design variables of the multi-objective optimisation problems.

Appendix C

This appendix provides computational performance metrics for the solution of the single- and multi-objective problems.

Table C1
Computational performance of the proposed algorithm in solving the CI and OPEX single-objective optimisation problems for 100 genetic algorithm starts.

		CI problem			OPEX problem		
	pto	Average number of generations per start	Average number of fitness function calls per start	Average running time per start	Average number of generations per start	Average number of fitness function calls per start	Average running time per start
	[-]	[-]	[-]	[sec]	[-]	[-]	[sec]
Calm	no	40	8 003	252	41	8 334	300
Calm +25 %	no	37	7 450	232	45	9 132	379
Design	no	41	8 259	339	47	9 358	482
Vessel 1	no	38	7 637	322	47	9 498	532
Vessel 2	no	36	7 349	572	47	9 420	1 015
Vessel 3	no	40	7 991	876	49	9 768	1 360
Calm	yes	38	7 680	225	51	10 326	439
Calm +25 %	yes	39	7 942	273	55	11 059	559
Design	yes	37	7 536	308	48	9 638	413
Vessel 1	yes	38	7 644	315	55	10 954	772
Vessel 2	yes	37	7 566	734	46	9 191	1 103
Vessel 3	yes	37	7 493	659	49	9 839	532

Table C2
Computational performance of the proposed algorithm in solving the multi-objective optimisation problem for 50 genetic algorithm starts.

	Weights				Average number of generations per start	Average number of fitness function calls per start	Average running time per start
	λ_1 [-]	λ_2 [-]	λ_3 [-]	λ_4 [-]	[-]	[-]	[min]
-	1.000	0.000	0.000	0.000	37	7 485	21
-	0.000	1.000	0.000	0.000	54	10 940	16
-	0.000	0.000	1.000	0.000	69	13 872	18
1	0.100	0.900	0.000	0.000	57	11 366	19
2	0.087	0.783	0.130	0.000	53	10 656	20
3	0.071	0.643	0.286	0.000	43	8 710	20
4	0.059	0.529	0.412	0.000	48	9 723	26
5	0.040	0.360	0.600	0.000	60	11 937	29
6	0.200	0.800	0.000	0.000	56	11 244	28
7	0.174	0.696	0.130	0.000	53	10 676	49
8	0.143	0.571	0.286	0.000	42	8 490	28
9	0.118	0.471	0.412	0.000	45	9 108	23
10	0.080	0.320	0.600	0.000	56	11 291	18
11	0.300	0.700	0.000	0.000	57	11 445	19
12	0.261	0.609	0.130	0.000	53	10 558	26
13	0.214	0.500	0.286	0.000	46	9 285	26
14	0.176	0.412	0.412	0.000	52	10 357	25
15	0.120	0.280	0.600	0.000	57	11 397	29
16	0.350	0.650	0.000	0.000	53	10 594	48
17	0.304	0.565	0.130	0.000	50	10 054	32
18	0.250	0.464	0.286	0.000	45	9 096	22
19	0.206	0.382	0.412	0.000	52	10 456	16
20	0.140	0.260	0.600	0.000	58	11 669	20
21	0.400	0.600	0.000	0.000	54	10 759	25
22	0.348	0.522	0.130	0.000	50	10 136	28
23	0.286	0.429	0.286	0.000	48	9 719	23
24	0.235	0.353	0.412	0.000	47	9 549	22
25	0.160	0.240	0.600	0.000	56	11 322	49
26	0.450	0.550	0.000	0.000	50	10 144	32
27	0.391	0.478	0.130	0.000	49	9 916	23
28	0.321	0.393	0.286	0.000	44	8 773	22
29	0.265	0.324	0.412	0.000	50	10 081	34
30	0.180	0.220	0.600	0.000	56	11 295	51
31	0.500	0.500	0.000	0.000	52	10 424	30
32	0.435	0.435	0.130	0.000	48	9 671	19
33	0.357	0.357	0.286	0.000	46	9 270	19
34	0.294	0.294	0.412	0.000	51	10 314	47
35	0.200	0.200	0.600	0.000	59	11 799	37

(continues on next page)

Table C2 *(continues from previous page)*

	Weights				Average number of generations per start	Average number of fitness function calls per start	Average running time per start
	λ_1 [-]	λ_2 [-]	λ_3 [-]	λ_4 [-]	[-]	[-]	[min]
36	0.550	0.450	0.000	0.000	52	10 353	20
37	0.478	0.391	0.130	0.000	49	9 829	24
38	0.393	0.321	0.286	0.000	46	9 278	31
39	0.324	0.265	0.412	0.000	54	10 921	49
40	0.220	0.180	0.600	0.000	60	12 103	35
41	0.600	0.400	0.000	0.000	52	10 389	18
42	0.522	0.348	0.130	0.000	44	8 935	19
43	0.429	0.286	0.286	0.000	46	9 278	27
44	0.353	0.235	0.412	0.000	52	10 361	22
45	0.240	0.160	0.600	0.000	59	11 772	24
46	0.650	0.350	0.000	0.000	51	10 200	21
47	0.565	0.304	0.130	0.000	45	9 081	25
48	0.464	0.250	0.286	0.000	48	9 597	24
49	0.382	0.206	0.412	0.000	54	10 755	26
50	0.260	0.140	0.600	0.000	57	11 500	30
51	0.700	0.300	0.000	0.000	48	9 597	20
52	0.609	0.261	0.130	0.000	45	9 084	13
53	0.500	0.214	0.286	0.000	49	9 766	14
54	0.412	0.176	0.412	0.000	53	10 562	13
55	0.280	0.120	0.600	0.000	60	12 024	57
56	0.750	0.250	0.000	0.000	47	9 553	39
57	0.652	0.217	0.130	0.000	44	8 951	42
58	0.536	0.179	0.286	0.000	47	9 518	21
59	0.441	0.147	0.412	0.000	54	10 885	16
60	0.300	0.100	0.600	0.000	61	12 170	17
61	0.800	0.200	0.000	0.000	45	9 053	29
62	0.696	0.174	0.130	0.000	48	9 747	24
63	0.571	0.143	0.286	0.000	49	9 869	19
64	0.471	0.118	0.412	0.000	55	10 948	52
65	0.320	0.080	0.600	0.000	55	11 086	45
66	0.850	0.150	0.000	0.000	47	9 400	43
67	0.739	0.130	0.130	0.000	48	9 593	12
68	0.607	0.107	0.286	0.000	49	9 896	12
69	0.500	0.088	0.412	0.000	51	10 318	33
70	0.340	0.060	0.600	0.000	60	12 055	27
71	0.900	0.100	0.000	0.000	43	8 746	25
72	0.783	0.087	0.130	0.000	49	9 766	26
73	0.643	0.071	0.286	0.000	52	10 452	24
74	0.529	0.059	0.412	0.000	53	10 574	25
75	0.360	0.040	0.600	0.000	60	12 063	36
76	0.950	0.050	0.000	0.000	41	8 210	14
77	0.826	0.043	0.130	0.000	43	8 643	26
78	0.679	0.036	0.286	0.000	49	9 872	25
79	0.559	0.029	0.412	0.000	55	11 074	27
80	0.380	0.020	0.600	0.000	65	12 973	36

Data availability

The data that has been used is confidential.

References

[1] Review of maritime transport. United Nations Conference on Trade and Development, 2022.

[2] Resolution MEPC.304(72) ANNEX 11 Initial IMO strategy on reduction of GHG emissions from ships, 2018.

[3] Resolution MEPC.377(80) ANNEX 15 2023 IMO Strategy on reduction of GHG emissions from ships, 2023.

[4] R. D. Geertsma, R. R. Negenborn, K. Visser, J. J. Hopman. Design and control of hybrid power and propulsion systems for smart ships: A review of developments. Applied Energy, 194: 30–54, 2017. https://doi.org/10.1016/j.apenergy.2017.02.060.

[5] I. Georgescu, M. Godjevac, K. Visser. Efficiency constraints of energy storage for on-board power systems. Ocean Engineering, 162: 239–247, 2018. https://doi.org/10.1016/j.oceaneng.2018.05.004.

[6] Resolution MEPC.245(66) ANNEX 5 Guidelines on the method of calculation of the attained energy efficiency design index (EEDI) for new ships, 2014.

[7] E. Lindstad, H. Borgen, G.S. Eskeland, C. Paalson, H. Psaraftis, O. Turan. The need to amend IMO's EEDI to include a threshold for performance in waves (realistic sea conditions) to achieve the desired GHG reductions. Sustainability, 11 (13): 3668, 2019. https://doi.org/10.3390/su11133668.

[8] N. L. Trivyza, A. Rentizelas, G. Theotokatos. A comparative analysis of EEDI versus lifetime CO2 emissions. Journal of Marine Science and Engineering, 8 (1): 61, 2020. https://doi.org/10.3390/jmse8010061.

[9] ECE/TRANS/WP.29/2020/77 Proposal for a new UN Regulation on uniform provisions concerning the approval of light duty passenger and commercial vehicles with regards to criteria emissions, emissions of carbon dioxide and fuel consumption and/or the measurement of electric energy consumption and electric range (WLTC), 2020.

[10] Q. Cui, B. Chen. Aviation carbon transfer and compensation of international routes in africa from 2019 to 2021. Scientific Data, 10 (1): 306, 2023. https://doi.org/10.1038/s41597-023-02219-7.

[11] G. G. Dimopoulos, C. A. Frangopoulos. Optimization of energy systems based on evolutionary and social metaphors. Energy, 33 (2): 171–179, 2008. https://doi.org/10.1016/j.energy.2007.09.002.

[12] F. Baldi. Modelling, analysis and optimisation of ship energy systems. PhD thesis, Department of Shipping and Marine Technology, Chalmers University of Technology, 2016.

[13] A. Papanikolaou. Ship Design Methodologies of Preliminary Design. Springer, 2014. https://doi.org/10.1007/978-94-017-8751-2.

[14] A. Papanikolaou. Holistic ship design optimization. Computer-Aided Design, 42 (11): 1028–1044, 2010. https://doi.org/10.1016/j.cad.2009.07.002.

[15] J. Barreiro, S. Zaragoza, V. Diaz-Casas. Review of ship energy efficiency. Ocean Engineering, 257: 111594, 2022. https://doi.org/10.1016/j.oceaneng.2022.111594.

[16] M. Jaurola, A. Hedin, S. Tikkanen, K. Huhtala. Optimising design and power management in energy-efficient marine vessel power systems: a literature review. Journal of Marine Engineering & Technology, 18 (2): 92–101, 2019. https://doi.org/10.1080/20464177.2018.1505584.

[17] F. Mylonopoulos, H. Polinder, A. Coraddu. A comprehensive review of modeling and optimization methods for ship energy systems. IEEE Access, 11: 32697–32707, 2023. https://doi.org/10.1109/access.2023.3263719.

[18] N. L. Trivyza, A. Rentizelas, G. Theotokatos. A novel multi-objective decision support method for ship energy systems synthesis to enhance sustainability. Energy Conversion and Management, 168: 128–149, 2018. https://doi.org/10.1016/j.enconman.2018.04.020.
[19] W. Zhang, Y. He, N. Wu, F. Zhang, D. Lu, Z. Liu, R. Jing, Y. Zhao. Assessment of cruise ship decarbonization potential with alternative fuels based on milp model and cabin space limitation. Journal of Cleaner Production, 425: 138667, 2023. https://doi.org/10.1016/j.jclepro.2023.138667.
[20] A. Dotto, F. Satta, U. Campora. Energy, environmental and economic investigations of cruise ships powered by alternative fuels. Energy Conversion and Management, 285: 117011, 2023. https://doi.org/10.1016/j.enconman.2023.117011.
[21] I. Gypa, M. Jansson, K. Wolff, R. Bensow. Propeller optimization by interactive genetic algorithms and machine learning. Ship Technology Research, 70 (1): 56–71, 2021. https://doi.org/10.1080/09377255.2021.1973264.
[22] I. Gypa, M. Jansson, R. Gustafsson, S. Werner, R. Bensow. Controllable-pitch propeller design process for a wind-powered car-carrier optimising for total energy consumption. Ocean Engineering, 269: 113426, 2023. https://doi.org/10.1016/j.oceaneng.2022.113426.
[23] M. Tadros, M. Ventura, C. G. Soares. Optimization procedures for a twin controllable pitch propeller of a ROPAX ship at minimum fuel consumption. Journal of Marine Engineering & Technology, 22 (4): 167–175, 2022. https://doi.org/10.1080/20464177.2022.2106623.
[24] M. Tadros, M. Ventura, C. Guedes Soares. Optimization procedure to minimize fuel consumption of a four-stroke marine turbocharged diesel engine. Energy, 168: 897–908, 2019. https://doi.org/10.1016/j.energy.2018.11.146.
[25] F. Baldi, U. Larsen, C. Gabrielii. Comparison of different procedures for the optimisation of a combined Diesel engine and organic Rankine cycle system based on ship operational profile. Ocean Engineering, 110: 85–93, 2015. https://doi.org/10.1016/j.oceaneng.2015.09.037.
[26] G. N. Sakalis, C. A. Frangopoulos. Intertemporal optimization of synthesis, design and operation of integrated energy systems of ships: General method and application on a system with diesel main engines. Applied Energy, 226: 991–1008, Sep 2018. https://doi.org/10.1016/j.apenergy.2018.06.061.
[27] C. A. Frangopoulos. Recent developments and trends in optimization of energy systems. Energy, 164: 1011–1020, 2018. https://doi.org/10.1016/j.energy.2018.08.218.
[28] S. D. Chatzinikolaou, N. P. Ventikos. Holistic framework for studying ship air emissions in a life cycle perspective. Ocean Engineering, 110: 113–122, 2015. https://doi.org/10.1016/j.oceaneng.2015.05.042.
[29] N. Vasilikis, R. D. Geertsma, K. Visser. Operational data-driven energy performance assessment of ships: the case study of a naval vessel with hybrid propulsion. Journal of Marine Engineering and Technology, 2022. https://doi.org/10.1080/20464177.2022.2058690.
[30] M. A. Ancona, F. Baldi, M. Bianchi, L. Branchini, F. Melino, A. Peretto, J. Rosati. Efficiency improvement on a cruise ship: Load allocation optimization. Energy Conversion and Management, 164: 42–58, 2018. https://doi.org/10.1016/j.enconman.2018.02.080.
[31] K. Kim, G. Roh, W. Kim, K. Chun. A preliminary study on an alternative ship propulsion system fueled by ammonia environmental and economic assessments. Journal of Marine Science and Engineering, 8: 183, 2020. https://doi.org/10.3390/jmse8030183.
[32] M. Rivarolo, D. Rattazzi, L. Magistri, A.F. Massardo. Multi-criteria comparison of power generation and fuel storage solutions for maritime application. Energy Conversion and Management, 244: 114506, 2021. https://doi.org/10.1016/j.enconman.2021.114506.
[33] A. Souflis-Rigas, J. Pruyn, A. A. Kana. Characterization of methanol power and energy systems' uncertainties and evaluation of their impact on layout design. Journal of Marine Engineering & Technology, pages 1–13, 2025. https://doi.org/10.1080/20464177.2025.2462387.
[34] L. Nikolopoulos, E. Boulougouris. A novel method for the holistic, simulation driven ship design optimization under uncertainty in the big data era. Ocean Engineering, 218: 107634, 2020. https://doi.org/10.1016/j.oceaneng.2020.107634.
[35] C. A. Frangopoulos. Developments, trends, and challenges in optimization of ship energy systems. Applied Sciences, 10 (13): 4639, 2020. https://doi.org/10.3390/app10134639.
[36] G. A. Livanos, G. Theotokatos, D. N. Pagonis. Techno-economic investigation of alternative propulsion plants for Ferries and RoRo ships. Energy Conversion and Management, 79: 640–651, 2014. https://doi.org/10.1016/j.enconman.2013.12.050.
[37] N. Wu, F. Zhang, F. Zhang, C. Jiang, J. Lin, S. Xie, R. Jing, Y. Zhao. An integrated multi-objective optimization, evaluation, and decision-making method for ship energy system. Applied Energy, 373: 123917, 2024. https://doi.org/10.1016/j.apenergy.2024.123917.
[38] S. Solem, K. Fagerholt, S. O. Erikstad, Ø. Patricksson. Optimization of diesel electric machinery system configuration in conceptual ship design. Journal of Marine Science and Technology, 20 (3): 406–416, 2015. https://doi.org/10.1007/s00773-015-0307-4.
[39] J. Zhu, L. Chen, R. Miao. Optimization of sail-hybrid electric power system for ships considering correlated environmental uncertainties. Applied Energy, 391: 125862, 2025. https://doi.org/10.1016/j.apenergy.2025.125862.
[40] E. K. Dedes, D. A. Hudson, S. R. Turnock. Investigation of diesel hybrid systems for fuel oil reduction in slow speed ocean going ships. Energy, 114: 444–456, 2016. https://doi.org/10.1016/j.energy.2016.07.121.
[41] F. Balsamo, C. Capasso, D. Lauria, O. Veneri. Optimal design and energy management of hybrid storage systems for marine propulsion applications. Applied Energy, 278: 115629, 2020. https://doi.org/10.1016/j.apenergy.2020.115629.
[42] J. Zhu, L. Chen, B. Wang, L. Xia. Optimal design of a hybrid electric propulsive system for an anchor handling tug supply vessel. Applied Energy, 226: 423–436, 2018. https://doi.org/10.1016/j.apenergy.2018.05.131.
[43] J. Zhu, L. Chen, L. Xia, B. Wang. Bi-objective optimal design of plug-in hybrid electric propulsion system for ships. Energy, 177: 247–261, 2019. https://doi.org/10.1016/j.energy.2019.04.079.
[44] X. Wang, U. Shipurkar, A. Haseltalab, H. Polinder, F. Claeys, R. R. Negenborn. Sizing and control of a hybrid ship propulsion system using multi-objective double-layer optimization. IEEE Access, 9: 72587–72601, 2021. https://doi.org/10.1109/access.2021.3080195.
[45] A. Dotto, F. Satta. Techno-economic optimization of hybrid-electric power plants onboard cruise ships. Energy Conversion and Management: X, 20: 100436, 2023. https://doi.org/10.1016/j.ecmx.2023.100436.
[46] G. Shu, P. Liu, H. Tian, X. Wang, D. Jing. Operational profile based thermal-economic analysis on an organic rankine cycle using for harvesting marine engine's exhaust waste heat. Energy Conversion and Management, 146: 107–123, 2017. https://doi.org/10.1016/j.enconman.2017.04.099.
[47] M. Tadros, M. Ventura, C. G. Soares. A nonlinear optimization tool to simulate a marine propulsion system for ship conceptual design. Ocean Engineering, 210: 107417, 2020. https://doi.org/10.1016/j.oceaneng.2020.107417.
[48] D. Peri. Robust design optimization for the refit of a cargo ship using real seagoing data. Ocean Engineering, 123: 103–115, 2016. https://doi.org/10.1016/j.oceaneng.2016.06.029.
[49] M. Diez, E. F. Campana, F. Stern. Stochastic optimization methods for ship resistance and operational efficiency via CFD. Structural and Multidisciplinary Optimization, 57 (2): 735–758, 2018. https://doi.org/10.1007/s00158-017-1775-4.
[50] M. Diez, D. Peri. Robust optimization for ship conceptual design. Ocean Engineering, 37 (11–12): 966–977, 2010. https://doi.org/10.1016/j.oceaneng.2010.03.010.
[51] E. Esmailian, S. Steen, K. Koushan. Ship design for real sea states under uncertainty. Ocean Engineering, 266: 113127, 2022. https://doi.org/10.1016/j.oceaneng.2022.113127.
[52] E. Esmailian, S. Steen. A new method for optimal ship design in real sea states using the ship power profile. Ocean Engineering, 259: 111893, 2022. https://doi.org/10.1016/j.oceaneng.2022.111893.
[53] A. Vrijdag, E. J. Boonen, M. Lehne. Effect of uncertainty on techno-economic trade-off studies: ship power and propulsion concepts. Journal of Marine Engineering & Technology, 18 (3): 122–133, 2018. https://doi.org/10.1080/20464177.2018.1507430.
[54] F. Tillig, J. W. Ringsberg, W. Mao, B. Ramne. Analysis of uncertainties in the prediction of ships' fuel consumption –from early design to operation conditions. Ships and Offshore Structures, 13 (sup1): 13–24, 2018. https://doi.org/10.1080/17445302.2018.1425519.
[55] K. Kim, M. R. von Spakovsky, M. Wang, D. J. Nelson. A hybrid multi-level optimization approach for the dynamic synthesis/design and operation/control under uncertainty of a fuel cell system. Energy, 36 (6): 3933–3943, 2011. https://doi.org/10.1016/j.energy.2010.08.024.
[56] J. P. Skeete. Examining the role of policy design and policy interaction in EU automotive emissions performance gaps. Energy Policy, 104: 373–381, 2017. https://doi.org/10.1016/j.enpol.2017.02.018.
[57] G. Fontaras, N. G. Zacharof, B. Ciuffo. Fuel consumption and CO2 emissions from passenger cars in europe –laboratory versus real-world emissions. Progress in Energy and Combustion Science, 60: 97–131, 2017. https://doi.org/10.1016/j.pecs.2016.12.004.
[58] J. L. Jiménez, J. Valido, N. Molden. The drivers behind differences between official and actual vehicle efficiency and CO2 emissions. Transportation Research Part D: Transport and Environment, 67: 628–641, 2019. https://doi.org/10.1016/j.trd.2019.01.016.
[59] M. Pfriem, F. Gauterin. Development of real-world Driving Cycles for Battery Electric Vehicles. In World Electric Vehicle Journal 8, 2016.
[60] I. Pagoni, V. Psaraki-Kalouptsidi. Calculation of aircraft fuel consumption and co2 emissions based on path profile estimation by clustering and registration. Transportation Research Part D: Transport and Environment, 54: 172–190, 2017. https://doi.org/10.1016/j.trd.2017.05.006.
[61] Q. Cui, Y. Lei, Y. Li. Protocol to calculate aircraft emissions for international air routes in South America. STAR Protocols, 4 (1): 101952, 2023. https://doi.org/10.1016/j.xpro.2022.101952.
[62] A. Godet, J. N. Nurup, J. T. Saber, G. Panagakos, M. B. Barfod. Operational cycles for maritime transportation: A benchmarking tool for ship energy efficiency. Transportation Research Part D: Transport and Environment, 121: 103840, 2023. https://doi.org/10.1016/j.trd.2023.103840.
[63] A. Godet, G. Panagakos, M. B. Barfod, E. Lindstad. Operational cycles for maritime transportation: Consolidated methodology and assessments. Transportation Research Part D: Transport and Environment, 132: 104238, 2024. https://doi.org/10.1016/j.trd.2024.104238.
[64] M. Duan, Y. Wang, A. Fan, J. Yang, X. Fan. Comprehensive analysis and evaluation of ship energy efficiency practices. Ocean & Coastal Management, 231: 106397, 2023. https://doi.org/10.1016/j.ocecoaman.2022.106397.
[65] N. Vasilikis, R. D. Geertsma, A. Coraddu. A digital twin approach for maritime carbon intensity evaluation accounting for operational and environmental uncertainty. Ocean Engineering, 288: 115927, 2023. https://doi.org/10.1016/j.oceaneng.2023.115927.
[66] MAN Energy solutions. Marine engine programme, 2023.
[67] Wärtsilä. Wärtsilä solutions for marine and oil & gas markets, 2023.
[68] Resolution MEPC.203(62) ANNEX 19 Amendments to the annex of the protocol of 1997 to amend the international convention for the prevention of pollution from ships, 1973, as modified by the protocol of 1978 relating thereto, 2011.

[69] P. Karagiannidis, N. Themelis. Data-driven modelling of ship propulsion and the effect of data pre-processing on the prediction of ship fuel consumption and speed loss. Ocean Engineering, page 108616, 2021. https://doi.org/10.1016/j.oceaneng.2021.108616.
[70] L. A. Roald, D. Pozo, A. Papavasiliou, D. K. Molzahn, J. Kazempour, A. Conejo. Power systems optimization under uncertainty: A review of methods and applications. Electric Power Systems Research, 214: 108725, 2023. https://doi.org/10.1016/j.epsr.2022.108725.
[71] M. Kalikatzarakis, R. D. Geertsma, E. J. Boonen, K. Visser, R. R. Negenborn. Ship energy management for hybrid propulsion and power supply with shore charging. Control Engineering Practice, 76: 133–154, 2018. https://doi.org/10.1016/j.conengprac.2018.04.009.
[72] J. Granacher. Overcoming decision paralysis—a digital twin for decision making in energy system design. volume 306, page 117954, 2022. https://doi.org/10.1016/j.apenergy.2021.117954.
[73] M. T. M. Emmerich, A. H. Deutz. A tutorial on multiobjective optimization: fundamentals and evolutionary methods. Natural Computing, 17 (3): 585–609, 2018. https://doi.org/10.1007/s11047-018-9685-y.
[74] N. V. Sahinidis. Mixed-integer nonlinear programming 2018. Optimization and Engineering, 20 (2): 301–306, 2019. https://doi.org/10.1007/s11081-019-09438-1.
[75] W. Stoecker. Design of thermal systems. McGraw-Hill Science/Engineering, 1989.
[76] A. Ravindran, K. M. Ragsdell, G. V. Reklaitis. Engineering Optimization. John Wiley & Sons, 2006.
[77] C. A. Frangopoulos, editor. Cogeneration: Technologies, Optimisation and Implementation, volume 87 of Energy Engineering Series. The Institution of Engineering and Technology, 2017.
[78] M. Sakawa. Genetic algorithms and fuzzy multiobjective optimization. Springer science and business media, LLC, 2002. https://doi.org/10.1007/978-1-4615-1519-7.
[79] M. J. Kochenderfer. Algorithms for optimization. The MIT Press, Cambridge, 2019.
[80] D. H. Wolpert, W. G. Macready. No free lunch theorems for optimization. IEEE Transactions on Evolutionary Computation, 1 (1): 67–82, 1997. https://doi.org/10.1109/4235.585893.
[81] A. R. Jordehi. A review on constraint handling strategies in particle swarm optimisation. Neural Computing and Applications, 26 (6): 1265–1275, 2015. https://doi.org/10.1007/s00521-014-1808-5.
[82] R. Martí. Multi-Start Methods, pages 355–368, Springer US: Boston MA, 2003, https://doi.org/10.1007/0-306-48056-5_12.
[83] K. Deb, A. Pratap, S. Agarwal, T. Meyarivan. A fast and elitist multiobjective genetic algorithm: NSGA-II. IEEE Transactions on Evolutionary Computation, 6 (2): 182–197, 2002. https://doi.org/10.1109/4235.996017.
[84] A. Coraddu, S. Gaggero, D. Villa, L. Oneto. A non-deterministic propeller design optimization framework leveraging machine learning based boundary element methods surrogates. In 10th Conference on Computational Methods in Marine Engineering (MARINE), 2023. https://doi.org/10.23967/marine.2023.139.
[85] Delft High Performance Computing Centre (DHPC). DelftBlue Supercomputer (Phase 1), 2022. https://www.tudelft.nl/dhpc/ark:/44463/DelftBluePhase1.